Available online at www.sciencedirect.com
ScienceDirect
Sedimentary Geology 202 (2007) 538–561
Sedimentary Geology
www.elsevier.com/locate/sedgeo

Coupled changes in sand grain size and sand transport driven by changes in the upstream supply of sand in the Colorado River: Relative importance of changes in bed-sand grain size and bed-sand area

D.J. Topping [a,*], D.M. Rubin [b], T.S. Melis [a]

[a] U.S. Geological Survey, 2255 N. Gemini Dr., Flagstaff, AZ 86001, USA
[b] U.S. Geological Survey, 400 Natural Bridges Dr., Santa Cruz, CA 95060, USA

Abstract

Sand transport in the Colorado River in Marble and Grand canyons was naturally limited by the upstream supply of sand. Prior to the 1963 closure of Glen Canyon Dam, the river exhibited the following four effects of sand supply limitation: (1) hysteresis in sediment concentration, (2) hysteresis in sediment grain size coupled to the hysteresis in sediment concentration, (3) production of inversely graded flood deposits, and (4) development or modification of a lag between the time of a flood peak and the time of either maximum or minimum (depending on reach geometry) bed elevation. Construction and operation of the dam has enhanced the degree to which the first two of these four effects are evident, and has not affected the degree to which the last two effects of sand supply limitation are evident in the Colorado River in Marble and Grand canyons. The first three of the effects involve coupled changes in suspended-sand concentration and grain size that are controlled by changes in the upstream supply of sand. During tributary floods, sand on the bed of the Colorado River fines; this causes the suspended sand to fine and the suspended-sand concentration to increase, even when the discharge of water remains constant. Subsequently, the bed is winnowed of finer sand, the suspended sand coarsens, and the suspended-sand concentration decreases independently of discharge. Also associated with these changes in sand supply are changes in the fraction of the bed that is covered by sand. Thus, suspended-sand concentration in the Colorado River is likely regulated by both changes in the bed-sand grain size and changes in the bed-sand area. A physically based flow and suspended-sediment transport model is developed, tested, and applied to data from the Colorado River to evaluate the relative importance of changes in the bed-sand grain size and changes in the bed-sand area in regulating suspended-sand concentration. Although the model was developed using approximations for steady, uniform flow, and other simplifications that are not met in the Colorado River, the results nevertheless support the idea that changes in bed-sand grain size are much more important than changes in bed-sand area in regulating the concentration of suspended sand.
Published by Elsevier B.V.

Keywords: Sand; Grain size; Suspended sediment; Supply limitation; Colorado River; Grand Canyon

1. Introduction

A reach of a river will be supply limited with respect to a certain sediment grain size over a chosen timescale

* Corresponding author. Tel.: +1 928 556 7445.
E-mail address: dtopping@usgs.gov (D.J. Topping).

0037-0738/$ - see front matter. Published by Elsevier B.V.
doi:10.1016/j.sedgeo.2007.03.016

if, over that timescale, the river has the capacity to transport more of that size class of sediment than is supplied (Topping et al., 2000a). By this definition, most rivers are expected to be supply limited with respect to some portion of the grain sizes of sediment in transport. Furthermore, this definition does not require that a supply-limited river is net erosional; deposition of coarser sizes may occur even if the river is supply limited with respect to the finer sizes in transport. Four coupled effects may be evident in a reach that is supply limited with respect to a specified size class of sediment over a given timescale (Topping et al., 2000a). The first three of these effects involve temporal changes in sediment concentration and grain size.

First, within the timescale over which a reach is supply limited, hysteresis in the suspended-sediment concentration of the supply-limited size class will result. Following sediment-supplying events to this reach, the concentration of the supply-limited size class will initially increase independently of the discharge of water, then subsequently decrease as that size class becomes depleted.

Second, associated with this hysteresis in suspended-sediment concentration, hysteresis will also exist in sediment grain size. This second effect results from the physical linkage between particle settling velocity and suspended-sediment transport (e.g., Rouse, 1937; Hunt, 1969; Smith, 1977; McLean, 1992). Because finer sizes have lower settling velocities than coarser sizes, the vertical gradient in sediment concentration is inversely related to particle size. Therefore, given that downstream velocity increases away from the bed, the transport rate of finer sediment in suspension will be greater than that of coarser sediment. Thus, when a finite quantity of sediment is supplied to a supply-limited reach, it will travel downstream as an elongating "sediment wave", with the finest sizes traveling the fastest. This sediment wave will have a component in the bed, the bedload, and the suspended load. As the front of a sediment wave passes a given location, the sediment-transport rate will first increase as the grain size of sediment on the bed fines, and will subsequently decrease as the bed sediment is winnowed (Topping et al., 2000b). This effect can occur independently of changes in the discharge of water.

The third effect of sediment supply limitation follows directly from the second effect. Because the grain size of sediment in suspension will coarsen over time during floods passing through a supply-limited reach, the sediment available for deposition on floodplains, on channel margins, or in eddies will coarsen through time. Thus, deposits produced during floods passing through a supply-limited reach will coarsen upward (Rubin et al., 1998; Topping et al., 1999).

The fourth effect of sediment supply limitation is the development or modification of a lag between the time of a flood peak and the time of either maximum or minimum (depending on reach geometry) bed elevation, and is described in detail in Topping et al. (2000a). Recent work has shown that the Colorado River in Marble and Grand canyons (Fig. 1) has exhibited these effects of sediment supply limitation both prior to and after the 1963 completion of Glen Canyon Dam (located 26.6 km upstream from the head of Marble Canyon and the upstream boundary of Grand Canyon National Park), but to differing degrees (Topping et al., 2000a,b; Rubin and Topping, 2001; Rubin et al., 2002).

2. Purpose and scope

This paper reviews the grain-size related evidence for sand-supply limitation in the Colorado River and then describes the development, testing, and application of a physically based flow and sediment-transport model used to evaluate the relative importance of changes in bed-sand grain size and bed-sand area in the coupling between the bed sand and the suspended-sand concentration and grain size.

3. Methods

The work we present in this paper draws heavily on both analyses of historical flow and sediment-transport data collected by the U.S. Geological Survey (USGS), and also on fieldwork that we have conducted in the post-dam Colorado River in Marble and Grand canyons (Fig. 1). All raw historical USGS stage, discharge, bed-topography, bed-sediment, and sediment-transport data were retrieved for two key gaging stations on the Colorado River, the Lees Ferry gaging station (located immediately upstream from the head of Marble Canyon and 25 km downstream from Glen Canyon Dam) and the Grand Canyon gaging station (located 141 km downstream from the Lees Ferry gaging station). We collected suspended-sediment data at the Grand Canyon gaging station using a P-61 point-integrating suspended-sediment sampler, and D-77, D-96, and D-96-A1 depth-integrating suspended-sediment bag samplers (Edwards and Glysson, 1999; Federal Interagency Sedimentation Project, 2001, 2003). Bed-sediment data were collected using a BM-54 bed-material sampler and a pipe dredge. Pre- and post-dam flood deposits were sampled vertically for grain size in Marble and Grand canyons (Rubin et al., 1998; Topping et al., 1999, 2000a,b, 2006a).

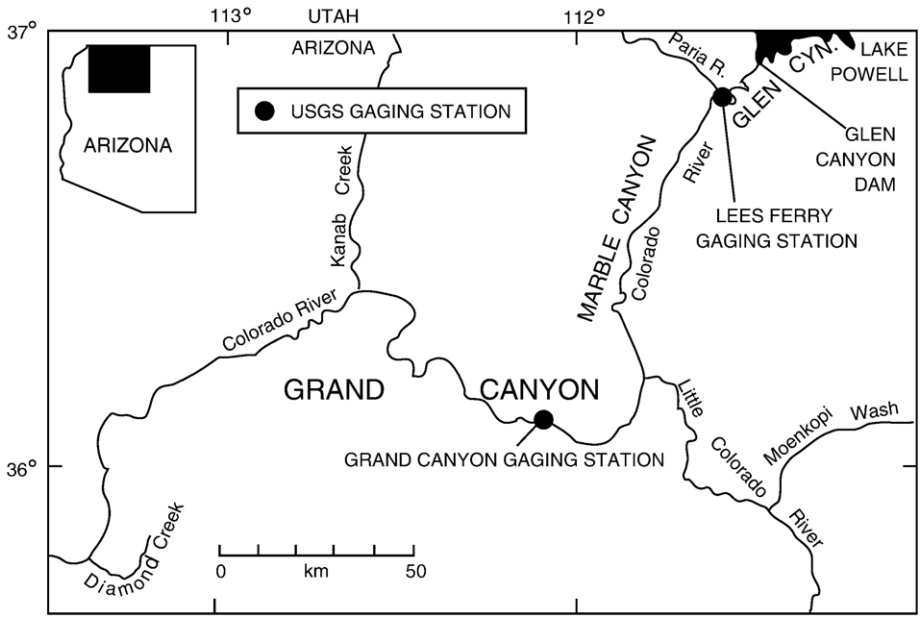

Fig. 1. Map of the study area showing the locations of the Lees Ferry gaging station (USGS station number 09380000) and Grand Canyon gaging station (USGS station number 09402500).

Grain-size distributions of the bed sediment and flood-deposit sediment were determined by dry sieving. Grain-size distributions of the pre-1999 USGS suspended-sand data were determined by either wet sieving or use of a visual accumulation tube. Grain-size distributions of the 1996 and 1998 P-61-sampler point measurements of the suspended sand were measured by use of a visual accumulation tube. Grain-size distributions of the post-1998 suspended-sand data were determined by use of a Beckman Coulter LS-100Q Laser Diffraction Particle Size Analyzer[1] calibrated to give the same results as dry sieving. The slope of the water surface at the Grand Canyon gaging station was measured at a variety of discharges in 1996 using a theodolite and stadia rod. Bedform geometries were measured in the reach at the Grand Canyon gaging station in 1996 using a boat-mounted single-beam sonar system.

4. Background

Changes in the upstream supply of sand have played a considerable role in regulating the rate of sand transport in the Colorado River in Marble and Grand canyons both prior to and after the completion of Glen Canyon Dam. Prior to dam closure in March 1963, the mean annual sand load of the Colorado River was approximately 25 to 26 million metric tons at the upstream boundary of Grand Canyon National Park at the head of Marble Canyon. Of this amount, approximately 24 million metric tons of sand were supplied from the Colorado River in Glen Canyon and 1.5 million metric tons of sand were supplied from the Paria River, the first major tributary located 26.5 km downstream from the site of Glen Canyon Dam (Topping et al., 2000a). Analysis of pre-dam sand-transport data from the Lees Ferry and Grand Canyon gaging stations (Fig. 1) and analysis of pre-dam sediment budgets for the reach between these gaging stations indicate that, during the average pre-dam year, between 1.7 and 13 million metric tons of sand accumulated in Marble Canyon and the part of Grand Canyon upstream from the Grand Canyon gaging station during the nine months of the year (July–March) when the discharge of the Colorado River was typically less than about 250 m^3/s. Then, during the three months of higher discharge during the annual snowmelt flood (April–June), this seasonally accumulated sand was eroded from this reach (Fig. 10 in Topping et al., 2000a). This annual pattern of nine months of sand accumulation and storage followed by three months of sand erosion led to substantial hysteresis in suspended-sand concentration and grain size, bed-sediment grain size, and bed elevation at the Grand Canyon gaging station. During the rising limb of the snowmelt flood, the following coupled effects of sand-supply limitation were observed at the Grand Canyon gaging station as the seasonally accumulated sand was depleted from the reach

[1] Use of brand and firm names in this paper does not constitute endorsement by the U.S. Geological Survey.

upstream: (1) the bed scoured (after initially aggrading), (2) the sand on the bed coarsened, (3) the suspended-sand coarsened, and (4) the suspended-sand concentration decreased (Topping et al., 2000a). The coarsening of the suspended sand during the snowmelt flood led to the production of inversely graded flood deposits in Marble and Grand canyons (Fig. 2).

Operation of Glen Canyon Dam has enhanced the effects of sand-supply limitation that operated in the natural Colorado River in Marble and Grand canyons. Construction of the dam reduced the supply of sand at the upstream boundary of Grand Canyon National Park by about 94% (i.e., the Paria River is now the only substantial supplier of sand) and operations of the dam have flattened the annual hydrograph (virtually eliminating the occurrence of both flood and base flows). Because of this change in the annual hydrograph, no season of sand accumulation exists in the post-dam river in Marble and Grand canyons. Side-scan-sonar data collected in 1984, 1994, 1996, 1998, 1999, and 2000 suggest that the majority of the bed of the Colorado River in Marble and Grand canyons is now composed of finer gravel, large immobile boulders, and bedrock, with only 20 to 40% of the bed composed of sand (Randle and Pemberton, 1987, analysis of 1984 data of Wilson, 1986; Anima et al., 1998; Wong et al., 2003; S. Goeking, Utah State University, unpublished 2004 analysis of 2000 data of R. Anima; R. Anima, written communication, 2006). Sand exists on the bed as sandbars in lateral recirculation eddies (e.g., Fig. 6 in Topping et al., 2005), in large patches on the channel bed, and as interstitial material in the gravel.

Recent research has shown that under the new dam-induced sand-supply and flow regime, changes in the upstream supply of sand due to both episodic tributary floods and changes in dam operations result in substantial discharge-independent changes in suspended-sand

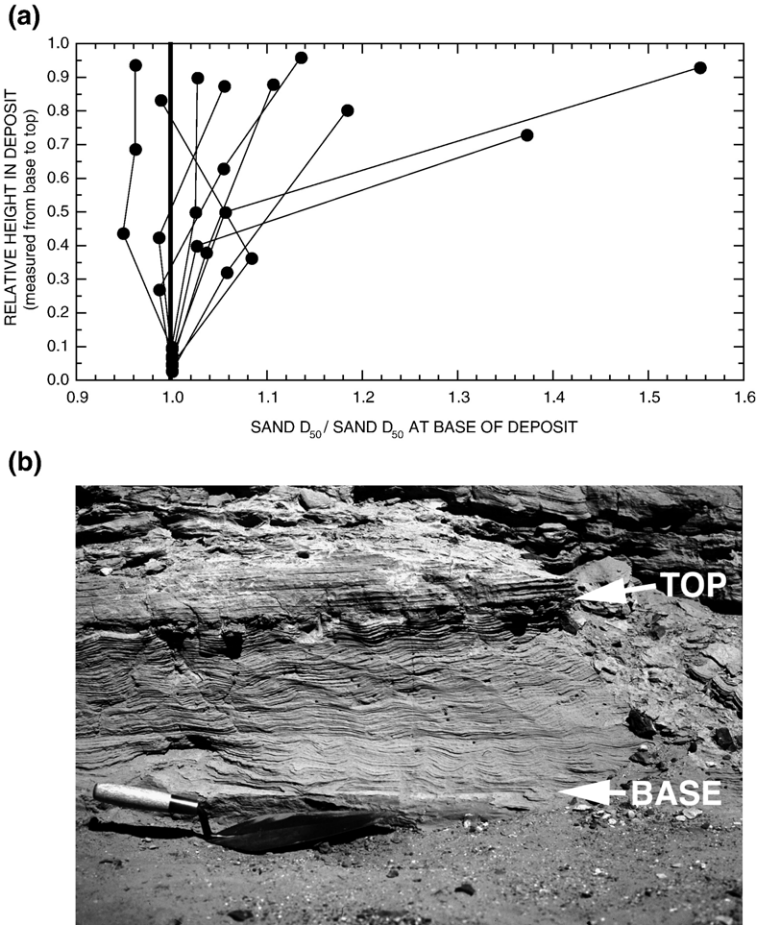

Fig. 2. a Vertical trends in the median grain size of sand in nine pre-dam flood deposits sampled in Marble and Grand canyons (after Topping et al., 2000a). The median grain size of the sand at each elevation in each flood deposit is normalized by the median grain size of the sand measured near the base. b Photograph of an inversely graded pre-dam flood deposit in Marble Canyon; base and top of deposit are indicated.

concentration coupled to changes in sand grain size (Topping et al., 2000b; Rubin and Topping, 2001; Topping et al., 2005, 2006a). In this type of supply-limited setting, stable relationships between the discharge of water and sand transport do not exist. The median size of the sand supplied by tributaries downstream from Glen Canyon Dam is about a factor of two to four finer than that typically comprising the sand on the bed of the channel of the Colorado River. Sand supplied during a tributary flood, therefore, causes short-term changes of a factor of four or more in the grain size of the sand on the bed. Following initial fining of the sand on the bed of the channel of the Colorado River during periods of tributary activity, the bed sand is winnowed in response to the depletion of the upstream supply of finer sand. Then, the suspended sand coarsens and suspended-sand concentrations decrease in response to the coarser bed sediment.

These factor of two to four changes in the grain size of the sand on the bed have a large effect on sand transport, the grain size of the sand in suspension supplied to depositional sites, and the configurations of the bedforms in these depositional sites. For typical flow conditions in the Colorado River, a factor of two change in the median size of the bed sand corresponds to a factor of 10 change in suspended-sand concentration, and a factor of four change in the median size of the bed sand corresponds to a factor of 100 change in suspended-sand concentration (Fig. 18 in Topping et al., 2000b). During higher dam releases, winnowing of the bed occurs rapidly as the upstream supply of sand is depleted (Fig. 4 in Topping et al., 2000b, 2006a). Thus, as during pre-dam floods, sand in suspension coarsens rapidly during post-dam floods, resulting in coarsening-upward flood deposits in Marble and Grand canyons (Fig. 3; Rubin et al., 1998; Topping et al., 1999, 2000b, 2005, 2006a). During an experimental flood released from Glen Canyon Dam in 1996 (Webb et al., 1999), this coarsening of the sand supply caused a change in bedform configuration from ripples to dunes at a number of depositional sites along the river (Rubin et al., 1998).

5. Analysis of suspended- and bed-sand data using a simple, physically based flow and sediment-transport model

To test whether the observed changes in suspended-sand concentration and grain size in the Colorado River could be explained predominantly by measured changes in the grain size of sand on the bed or whether changes

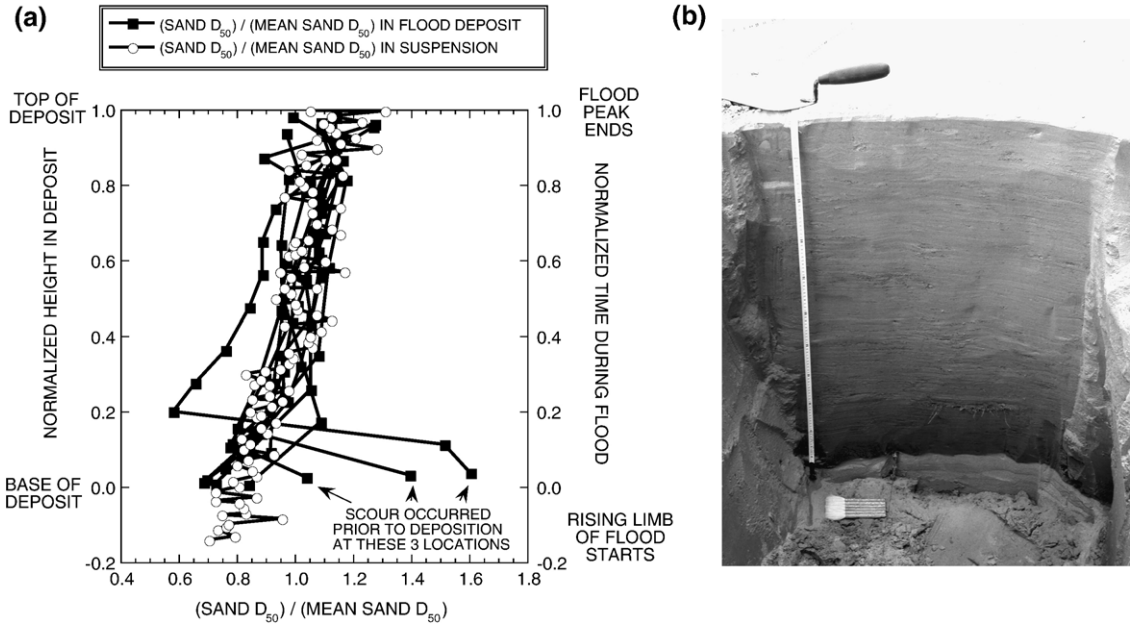

Fig. 3. a Comparison of the vertical trends in the median grain size of sand in flood deposits produced during an artificial flood released from Glen Canyon Dam in 2004 (i.e., the 2004 controlled flood) with the trend in the median grain size of suspended sand during the rising limb and peak of this flood (after Topping et al., 2006a). Deposits were sampled in the upstream half of Marble Canyon and the median size of the suspended sand was measured in the middle part of Marble Canyon. Median grain size of the sand at each elevation in each deposit is normalized by the mean median grain size of the sand in each deposit; median grain size of the sand in suspension is normalized by the mean median grain size of the sand in suspension during the flood. At the three indicated sites, scour preceded deposition and 2–10 cm of clean, horizontally laminated sand (with the same, coarser grain size as the underlying pre-flood bar surface) was deposited prior to the coarsening-upward part of the deposit. b Photograph of a 1.1-m-thick inversely graded flood deposit in Marble Canyon produced during the 2004 controlled flood; note the upright scour chain in the coarser clean sand underlying the deposit.

in the area of sand on the bed were also important, data from the Grand Canyon gaging station were analyzed using a physically based flow and suspended-sediment-transport model. For purposes of conducting these evaluations, the model was developed for equilibrium transport of suspended sediment (meaning zero net flux of sediment between suspension and the bed) using steady, uniform flow theory. Inputs to this model are (1) the water-surface stage, (2) the average of the grain-size distributions of the sand, silt, and clay (hereafter referred to as fine sediment) on the bed measured at three to five locations across the cross-section under the measurement cableway, and (3) the assumed fractional area of the bed that is covered by fine sediment (note that this third input is not measured). Outputs from this model are the discharge of water passing through the cross-section under the measurement cableway and (1) the velocity profile and (2) suspended-sediment-concentration profiles (for 10 $1/2-\phi$ size classes of sand and one size class of silt and clay) in the middle of the cross-section at the measurement cableway.

So that it is robust and portable, the physically based model developed herein is the simplest steady, uniform-flow velocity- and sediment-concentration-profile model. This model uses two key assumptions: (1) spatial averaging of flow and bed conditions is a physically legitmate method for simplifying the lower boundary conditions, and (2) although sand transport is unsteady in the Colorado River, bed grain size is treated as an independent variable because it changes much more slowly over time than the other dependent variables. This second assumption was used by Rubin and Topping (2001) and is based on Einstein and Chien (1953), who showed that bed grain size has a "strong and immediate" effect on the transport of bed sediment, whereas flow and sediment transport have "weak and slow" influences on bed grain size.

Following the first assumption above, the model uses spatial averaging to approximate uniform flow and bed conditions, a standard approach that has been applied successfully to other sediment-transport problems. In this particular problem, however, we are specifically interested in a situation in which flow is nonuniform and sediment is nonuniformly distributed, thereby departing from the conditions for which this model is completely valid.

Nonuniform flow and bed sediment can be expected to affect sediment transport in several ways, depending on how they are coupled spatially. Where grain size on the bed is uniform over the bed, mean suspended-sediment concentration in a reach would be enhanced as flow nonuniformity increases; for the same mean flow, greater nonuniformity requires a greater range in velocities, causing higher sediment concentrations. The expected increase in concentration might even be greater in situations where flow and bed grain size are spatially coupled. For example, if grain size of sediment in dune troughs (where flow is weak) is systematically coarser than at dune crests (where flow is stronger), the mean concentration can be expected to be greater than if bed-sediment grain size was uniform across the topography (e.g., if the gravel were equally mixed with the sand at all locations). This situation, where the bed grain size is "out of phase" with the flow, is common in the Colorado River in Marble and Grand canyons and elsewhere; it describes "starved" dunes migrating over a gravel substrate. Because grain size and flow are related in a nonlinear way to concentration, the mean concentration in these nonuniform situations might be expected to differ from the concentration calculated from spatially averaged mean values.

In at least one common situation, spatial coupling between flow and bed grain size might reduce the expected increase in suspended-sediment concentration arising from flow nonuniformity: where sediment on the bed is sorted spatially such that the finer sizes occur in regions of weaker flow (such as in the pools upstream from rapids or in the lateral recirculation eddies in a pool/drop river). In this second case, where the bed grain size is "in phase" with the flow, the combination of conditions that produces the highest suspended-sediment concentrations (e.g., if the finest grain sizes on the bed were in the strongest flow) is reduced or eliminated entirely. It is not coincidence that this combination of conditions is less likely to occur in nature; the high transport rate experienced by the finest grain sizes in the strongest flow makes this situation relatively less stable. The point of these examples (both of which typically occur in the Colorado River in Marble and Grand canyons) is to show the same spatially averaged mean conditions might lead to different suspended-sediment concentrations, depending on whether bed sediment is distributed uniformly relative to flow, or coupled out of phase (starved dunes) or in phase (pool/drop).

Even though the problem at hand involves nonuniform conditions, the boundary conditions (spatial distribution of bed sediment and flow) are not defined well enough to use any other approach. We therefore apply this model cautiously, and use it in an exploratory manner to assess how well it performs, and to guide our understanding of the relative importance of the areal coverage and grain size of suspendable bed sediment in regulating suspended-sediment concentration.

The velocity component of this model was tested against velocity-profile data collected on May 18, 1944 (at a discharge of 2300 m^3/s), during May 30 through

June 8, 1947 (at discharges of 1250–1450 m^3/s), during March 26 through April 3, 1996 (at discharges of 238, 790, and 1280 m^3/s), and on September 26, 1998 (at a discharge of 908 m^3/s). The ability of the model to accurately predict the discharge of water at the Grand Canyon gaging station was tested using the average stage-discharge rating curve fit to the 3703 pre-dam discharge measurements made by the USGS between November 12, 1922, and March 6, 1963 (Fig. 9d in Topping et al., 2003). The suspended-sand-concentration-profile component of the model was tested against concentration-profile data collected during May 30 through June 8, 1947, during March 28 through April 2, 1996, and on September 26, 1998. Following these tests, the model was used to calculate curves relating suspended-sand concentration and grain size to the discharge of water (i.e., sand rating curves) over the range of plausible fractional areas of fine sediment on the bed, using as input bed grain-size distributions measured during the pre- and post-dam eras at the Grand Canyon gaging station.

5.1. Governing equations

Because the flow is approximated as steady and uniform, the total boundary shear stress is

$$\tau_b = -\rho g h S_f \tag{1}$$

where ρ is the density of water, g the gravitational acceleration, h the flow depth, and S_f the friction slope. All model calculations are performed in cgs units; computed concentrations are dimensionless volume fractions (i.e., volumetric). In a uniform flow, the vertical distribution of the total stress is linear (e.g., Tennekes and Lumley, 1972; Middleton and Southard, 1984) such that

$$\tau_{zx}(z) = \tau_b\left(1 - \frac{z}{h}\right) \tag{2}$$

where $\tau_{zx}(z)$ is the total shear stress at each level z in the vertical. In the case of the Colorado River, the vertical distribution of the total shear stress must be modified in the lower portion of the flow because of the presence of dunes on the bed. The presence of dunes on the bed reduces the value of $\tau_{zx}(z)$ in the lower portion of the flow (e.g., Smith and McLean, 1977; Nelson et al., 1993). Thus, following the technique of Smith and McLean (1977), the total shear stress below the tops of the dunes is partitioned at each level z into a fluid component, i.e., a component related to the velocity and sediment transport, and into a form-drag component due to the presence of the dunes. At the bed, the fluid component of the stress, τ_f, is equal to the skin-friction stress, τ_{sf}, the stress related to entrainment of fine sediment from the bed into transport. Below the tops of the dunes, the fluid-stress profile is also approximated as linear:

$$\tau_f(z) = \tau_{sf}\left(1 - \frac{z}{h}\right) \tag{3}$$

The value of τ_{sf} is calculated by the Wiberg and Smith (1989) modification of the method of Smith and McLean (1977):

$$\tau_{sf} = \tau_b \Bigg/ \left\{1 + \frac{C_D}{2}\frac{H}{\lambda}\left[\frac{1}{k}\left(\ln\frac{H}{(z_0)_{sf}} - 1\right)\right]^2\right\} \tag{4}$$

where C_D=0.2 is the drag coefficient for separated flow over dunes (Smith and McLean, 1977; Nelson et al., 1993), H the height of the dune, λ the wavelength of the dune, k=0.408 is von Karman's constant (Long et al., 1993), and $(z_0)_{sf}$ the skin-friction bed roughness parameter (the bed roughness parameter that would exist if the dunes were not present). Based on single-beam-sonar observations of dune geometry in the reach at the Grand Canyon gaging station during flows ranging in discharge from 238 to 1280 m^3/s during March 26 through April 3, 1996 (Fig. 4), H/h, in this application of the model, is held constant at 0.05, and the ripple index, λ/H, is held constant at 25. The value of $(z_0)_{sf}$ is set equal to 0.2 cm. Rotating side-scan-sonar data collected by Rubin et al. (2001) indicate that the dunes on many of the sand patches on the bed of the Colorado River in Marble and Grand canyons are starved, with gravel exposed in the troughs. Bed-sediment samples collected at the measurement cableway at the Grand Canyon gaging station and in the reach upstream almost always contain some gravel. Because the bed of the Colorado River is composed of gravel and fine sediment, the value of $(z_0)_{sf}$ used in this model is therefore larger than if the bed were entirely composed of fine sediment, and the skin-friction bed roughness parameter were only related to either the thickness of the bedload layer (Wiberg and Rubin, 1989) or high near-bed concentrations of suspended sediment (Gelfenbaum and Smith, 1986; Topping, 1997).

To solve for the velocity profile, the following constitutive equation for steady, horizontally uniform flow is used to relate the fluid stress to the vertical gradient in the time-averaged velocity:

$$\tau_f(z) = \rho K(z)\frac{\partial \overline{u}}{\partial zq} \tag{5}$$

where $K(z)$ is the eddy viscosity, and $\overline{u}$ the time-averaged, streamwise velocity. The eddy viscosity varies as a function of the flow and characterizes the vertical exchange of momentum due to turbulence. In situations

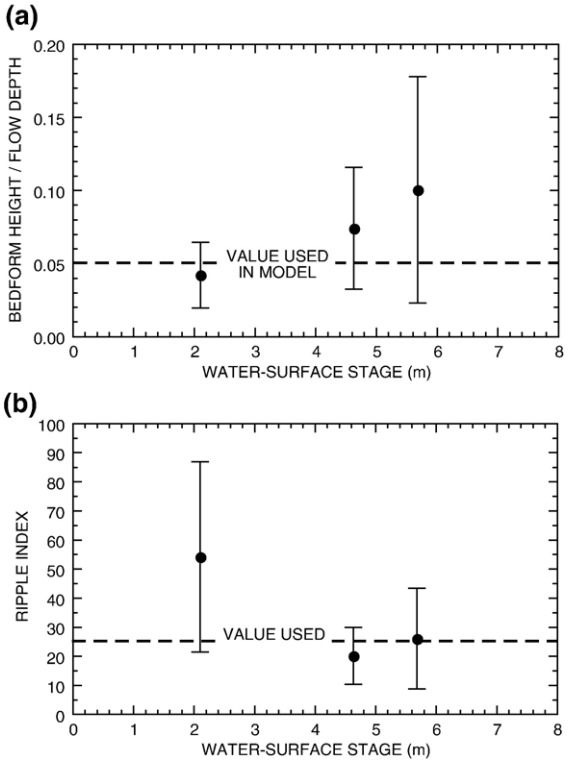

Fig. 4. Dune geometries measured using single-beam sonar in the reach at the Grand Canyon gaging station. Values at a water-surface stage of 2.05 m (discharge of 238 m^3/s) were calculated using the dimensions of 37 bedforms measured on March 26, 1996; values at a water-surface stage of 5.7 m (discharge of 1280 m^3/s) were calculated using the dimensions of 162 bedforms measured on March 27–April 2, 1996; values at a water-surface stage of 4.6 m (discharge of 906 m^3/s) were calculated using the dimensions of 37 bedforms measured on April 3, 1996. a Bedform height divided by depth of flow; error bars are one standard deviation. b Ripple index (bedform wavelength divided by the bedform height); error bars are one standard deviation.

where high density gradients (due to the presence of suspended sediment) occur in the flow, the eddy viscosity must be modified to account for the damping of turbulence (Monin and Yaglom, 1965; Smith and McLean, 1977; Gelfenbaum and Smith, 1986; McLean, 1991, 1992; Topping, 1997; Wright and Parker, 2004). However, in the Colorado River at the Grand Canyon gaging station, large boils shed frequently from dunes on the bed increase vertical mixing in the water column (process reviewed in Best, 2005) and are hypothesized to inhibit the formation of stable density-stratified flows. Therefore, the effect of density stratification is excluded and the eddy viscosity used in the model is the standard, clear-water two-part eddy viscosity of Rattray and Mitsuda (1974) where

$$K(z) = ku^*z\left(1-\frac{z}{h}\right) \quad \text{when } z\leq 0.2h \tag{6a}$$

and

$$K(z) = \frac{ku^*h}{\beta} \quad \text{when } z>0.2h \tag{6b}$$

where β=6.25 by the matching height of $0.2h$, and u^* is the shear velocity and is set equal to $\sqrt{\tau_b/\rho}$ in the interior of the flow and $\sqrt{\tau_{sf}/\rho}$ below the tops of the dunes. Finally, by inserting this eddy viscosity in Eq. (5), integrating Eq. (5) with respect to z, and rearranging terms, the following form of the velocity profile is obtained:

$$\overline{u}(z) = \frac{u^*}{k}\ln\left(\frac{z}{z_0}\right) \quad \text{when } z\leq 0.2h \tag{7a}$$

and

$$\overline{u}(z) = \frac{u^*\beta}{k}\left[\frac{z}{h}-\frac{(z/h)^2}{2}\right] + \frac{u^*}{k}\left[\ln\left(\frac{0.2}{z_0/h}\right)-1.123\right] \quad \text{when } z>0.2h \tag{7b}$$

Below the tops of the dunes, the bed roughness parameter, z_0, in Eqs. (7a) (7b) is equal to $(z_0)_{sf}$ and above the tops of the dunes, z_0 is determined by a rearranged version of Eq. (3) in Smith and McLean (1977):

$$z_0 = \frac{H/h}{\exp\left[\sqrt{\frac{\tau_{sf}}{\tau_b}}\ln\left(\frac{H/h}{(z_0)_{sf}}\right)\right]} \tag{8}$$

To accurately model suspended-sediment concentration profiles, multiple size classes of sediment must be included in the calculation (McLean, 1992). In the Colorado River case, where the goal is to accurately model both the equilibrium concentration and grain-size distribution of the suspended sand, 10 size classes of sand in equal $1/2-\phi$ increments (covering the grain-size range from 0.0625 to 2 mm) and one size class of silt and clay were included in the model (for the detailed derivation of the suspended-sediment concentration profile for each size class, see Eqs. (6)–(14) in McLean, 1992). Because, in this application of the model, the clear-water eddy viscosity is used and the effects of density stratification have been excluded, Eq. (14) in McLean (1992) simplifies to the following for each size-class m of sediment at each level z:

$$\left(\frac{\overline{c}_m}{1-\overline{c}_s}\right)_z = \left(\frac{\overline{c}_m}{1-\overline{c}_s}\right)_a\left[\left(\frac{a}{z}\right)\left(\frac{h-z}{h-a}\right)\right]^p \quad \text{when} \quad z\leq 0.2h \tag{9a}$$

and

$$\left(\frac{\overline{c}_m}{1-\overline{c}_s}\right)_z = \left(\frac{\overline{c}_m}{1-\overline{c}_s}\right)_a \left[\left(\frac{a}{0.2h}\right)\left(\frac{0.8h}{h-a}\right)\right]^p \times \exp\left[-p\frac{\beta}{h}(z-0.2h)\right] \quad \text{when } z>0.2h \tag{9b}$$

In Eqs. (9a) (9b), $\overline{c}_m$ is the time-averaged volumetric concentration of sediment in size-class m, $\overline{c}_s$ is the total concentration of sediment in all M size classes, a is the level at which the reference concentration is calculated (this level is different for the regions of the flow below and above the tops of the dunes), and p is the Rouse number. The Rouse number is given by

$$p = \frac{w_m}{ku^*} \tag{10}$$

where w_m is the settling velocity of sediment in size-class m, and again u^* is set equal to $\sqrt{\tau_b/\rho}$ in the interior of the flow and $\sqrt{\tau_{sf}/\rho}$ below the tops of the dunes. Settling velocities are calculated by the method of Dietrich (1982) for sediment with a Powers index of 3.0 and a Corey shape factor of 0.7; typical sediment from this site has a mean Powers index of 3.0 and a mean Corey shape factor of 0.7 (Topping, 1997). Water temperature was held constant at 15 °C, and clear-water fluid densities and viscosities were used in all calculations in the model. The level a, in the region where z is less than or equal to the elevation of the tops of the dunes, is set equal to the elevation of the top of the bedload layer, as calculated by Wiberg and Rubin (1989). In the region above the tops of the dunes, a is set equal to the elevation of the top of the dunes, and $\overline{c}_m$ and $\overline{c}_s$ at a are determined by Eq. (9a). In the region of the flow either at or below the elevation of the tops of the dunes, $\overline{c}_m$ and $\overline{c}_s$ at a are determined by the boundary condition described below.

Under conditions of nonequilibrium suspended-sediment transport, the correct form of the lower boundary condition for suspended sediment is the flux boundary condition developed by Parker (1978). For multiple size classes of sediment, the flux boundary condition becomes

$$K(z)\frac{\partial \overline{c}_m}{\partial z} = (\overline{c}_m)_a\left(\sum_{m=1}^{M}(\overline{c}_m W_m) - w_m\right) \tag{11}$$

where $(\overline{c}_m)_a$ is the near-bed, time-averaged concentration of suspended sediment in size-class m in local equilibrium with the grain-size distribution on the bed. The summation in Eq. (11) arises by conservation of mass from the upward flux of water driven by the downward settling of all M size classes of sediment. This boundary condition allows for the net flux of sediment in size class m from suspension to the bed when the bed contains less sediment in size class m than is required to support the amount of size class m present in suspension (this condition is typically referred to as overloading). Likewise, this boundary condition allows for the net flux of sediment in size class m from the bed to suspension when the bed contains more sediment in size class m than is required to support the amount of size class m present in suspension (this condition is typically referred to as underloading). This flux boundary condition thus provides the physical linkage between changes (over time and space) in the grain-size distribution of the bed and changes in the concentration and grain-size distribution of the suspended sediment.

In situations where the flow is steady and uniform, the bed is composed entirely of suspendable material and the suspended sediment is in equilibrium with the grain-size distribution on the bed (i.e., the zero-flux condition of Parker, 1978), the lower boundary condition for suspended sediment simplifies to a simple reference-concentration equation, such as the following linear form of the reference concentration of Smith and McLean (1977):

$$(\overline{c}_m)_a = i_m c_b \gamma S^* \tag{12}$$

where i_m is the volumetric fraction of sediment size-class m in the bed, $c_b = 0.65$ the volumetric concentration of fine sediment in the bed, and γ a constant set equal to 0.0045 (P. Wiberg, personal communication, 1989; McLean, 1992). S^* is the excess shear stress $(\tau_{sf}-\tau_{cr})/\tau_{cr}$ in which τ_{cr} is the critical shear stress for the median grain size of the fine-sediment mixture on the bed calculated by the method of Wiberg and Smith (1987) for a value of $d/k_s = 1$. The empirically determined constant γ sets the concentration at the top of the bedload layer for a given value of S^*. To preclude the occurrence of physically unrealistic high concentrations of suspended sediment, $(\overline{c}_m)_a$ is set equal to $0.5i_m$, when $(\overline{c}_s)_a$ is predicted to be greater than 0.5 by Eq. (12). This linear form of the Smith and McLean (1977) boundary condition has been found to work well in tests conducted by Topping (1997) against the entire range of conditions in the flume experiments of Kennedy (1961) and Guy et al. (1966), and the Rio Puerco measurements of Nordin (1963).

If the bed is not entirely composed of suspendable material, the lower boundary condition in Eq. (12) must be modified (e.g., McLean, 1992; Topping, 1997; Grams, 2006) or the amount of suspended sediment computed to be in equilibrium with a given fine-sediment mixture on the bed will be too large. To account for the fact that

suspendable material (i.e., fine sediment) comprises only a fraction of the bed of the Colorado River, Eq. (12) is therefore modified in the model as follows:

$$(c_m)_a = A_s i_m c_b \gamma S^* \quad (13)$$

where A_S is the fractional area of the bed that is covered by fine sediment, i_m therefore becomes the volumetric fraction of sediment size-class m in the part of the bed covered by fine sediment, and c_b=0.65 becomes the volumetric concentration of fine sediment in the part of the bed covered by fine sediment. In solving Eq. (13), we have only one independent measurement of A_S made simultaneously with flow, suspended-sediment, and bed-sediment measurements in our study reach, although we have additional constraints from side-scan-sonar mapping of the distribution of bed-sediment types (Anima et al., 1998; Wong et al., 2003; S. Goeking, Utah State University, unpublished 2004 analysis of 2000 data of R. Anima) of how A_S can vary there and elsewhere in Marble and Grand canyons. Consequently, our approach is to rearrange the terms in Eq. (13), and use measured concentrations to solve for A_S. In this usage, A_S is the only adjustable coefficient in the model and (as will be seen below), it becomes a "catch-all" term for any other errors in Eq. (13). A_S is the least well-constrained term and may also include physical processes other than those associated with changes in the area of fine sediment on the bed (as well as any of the processes mentioned above that couple flow to bed-sediment distribution).

There are two spatial scales that are important in determining the validity of A_S as a measure of the true areal coverage of fine sediment on the bed. The first of these spatial scales is the dimension of either the patches or the spaces between the patches of fine sediment. The second of these spatial scales is the length of the reach of river over which the suspended sediment equilibrates with the bed. We do not have a rigorous understanding

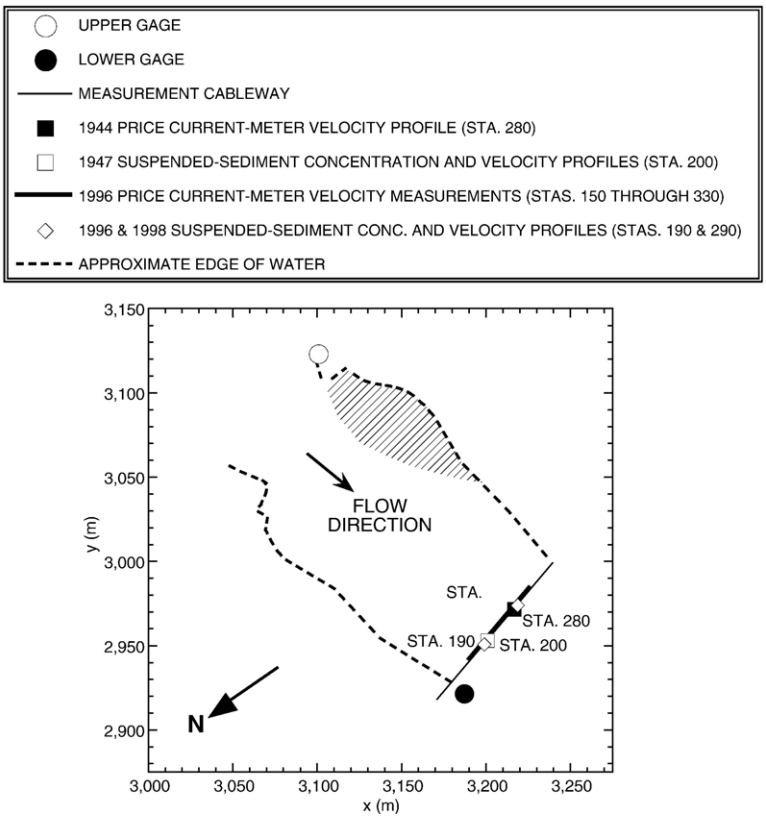

Fig. 5. Map of the reach at the Grand Canyon gaging station showing the locations of the upper and lower gages, the measurement cableway, the stations on the cableway at which velocity measurements were made in 1944, 1947, 1996, and 1998, and at which point suspended-sediment samples were collected in 1947, 1996, and 1998. Cableway stations are measured in feet from the right-bank endpoint. Cross-hatched area indicates the approximate location of a large lateral recirculation eddy on river left. X–y coordinate system is arbitrarily oriented; true north indicated by arrow.

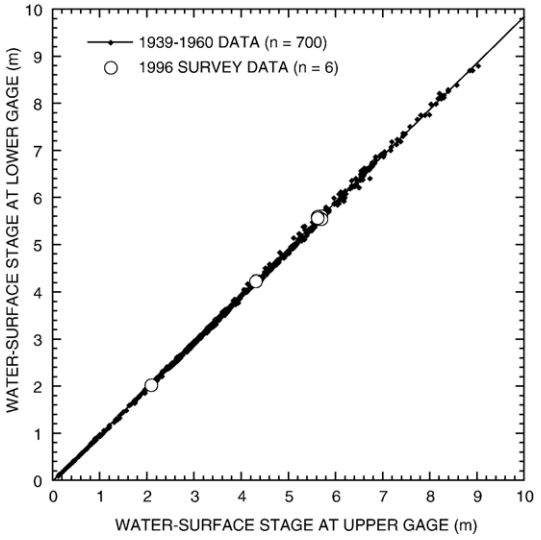

Fig. 6. Water-surface stage at the lower gage as a function of the water-surface stage at the upper gage based on 700 simultaneous observations of stage at these two gages made by the USGS between 1939 and 1960; solid line is the best-fit linear regression through these data (R^2=0.9995). Also shown are the measurements made during six topographic surveys of the water surface conducted between March 26 and April 3, 1996.

of how this first spatial scale affects the relation between A_S and the true areal coverage of fine sediment on the bed. However, the second spatial scale can be estimated by computing the streamwise distance required for the median grain size of the sediment in suspension to settle from near the surface of the flow to the bed. Given the range in settling velocities of the median grain size of the sand in suspension (0.5–1.5 cm/s), flow depths (400–900 cm), and mean velocities (70–300 cm/s) that exist at the measurement-cableway cross-section at the Grand Canyon gaging station, the spatial scale over which the suspended-sand equilibrates with the bed ranges from about 600 m to well over 1 km. This spatial scale is larger than the typical dimension of the patches of fine sediment on the bed of the Colorado River upstream from the Grand Canyon gaging station (Anima et al., 1998; Wong et al., 2003; S. Goeking, Utah State University, unpublished 2004 analysis of 2000 data of R. Anima; R. Anima, written communication, 2006). It is important to note that location of sand patches on the bed is not random but controlled primarily by hydraulics (i.e., the interaction of the flow with the local bed topography), and that changes in the upstream supply of sand affect the size of these patches but provide only a secondary control on the location of these sand patches on the bed (Topping et al., 2000b).

In the structure of this model, the effect of changing the fractional area of fine sediment on the bed is kept separate from the effect of changing the grain-size distribution of the fine sediment on the bed. By virtue of the physics in Eqs. (9a)–(13), a change in the fractional area of fine sediment on the bed will affect only the overall concentration of sediment in suspension, not the grain-size distribution of the sediment in suspension. Therefore, the grain-size distribution of the sediment in suspension can be changed only through a change in the grain-size distribution of the fine sediment on the bed.

5.2. Application of model to the geometry of the reach at the Grand Canyon gaging station

Friction slope in the reach at the Grand Canyon gaging station varies as a function of stage. Because two gages (upper and lower) are present in this reach (Fig. 5), with the upper gage providing the primary stage record, application of the model to the measurement-cableway cross-section at the Grand Canyon gaging station therefore required that flow depth and friction slope be determined as a function of stage at the upper gage. To simplify the model, the slightly trapezoidal cross-section at the cableway (Fig. 16a in Topping et al., 2000b) was treated as a 72-m-wide rectangle (with slip on the walls), and the pre-dam seasonal bed-elevation changes that occurred out of phase with changes in stage (depicted in Fig. 3 in Topping et al., 2000b) were averaged out. Thus, flow depth at the cableway cross-section, h, was related to stage at the lower gage, $h_{\text{lower gage}}$, by the following equation:

$$h = 280 + 0.9(h_{\text{lower gage}}) \quad (14)$$

Again, all calculations are performed in cgs units. Analysis of simultaneous observations of stage at

Fig. 7. Measured and model-predicted velocity profiles; also shown are the discharge of water (Q), and the measured and model-predicted mean velocities over the elevation range of the measurements. a On May 18, 1944; model-predicted mean velocity is 3% lower than that measured using the Price current meter. b On May 30–June 8, 1947; model-predicted mean velocity is 13% lower than that measured using the Price current meter and 8% lower than that measured using the P-46 point-integrating suspended-sediment sampler. c On March 26, 1996; model-predicted mean velocity (211 cm/s) is 0.3% lower than that measured using the Price current meter. d On March 27–April 2, 1996; model-predicted mean velocity over the elevation range of the current-meter measurements is 8% lower than that measured using the Price current meter and the model-predicted mean velocity (200 cm/s) over the elevation range of the P-61 measurements is 5% lower than that measured using the P-46 point-integrating suspended-sediment sampler. e On April 3, 1996; model-predicted mean velocity is 1% lower than that measured using the Price current meter. f On September 26, 1998; model-predicted mean velocity is 16% higher than that measured using the P-61 point-integrating suspended-sediment sampler.

the upper and lower gages during 1939–1960 and during 1996 (Fig. 6) indicated that the relationship of stage at the lower gage relative to stage at the upper gage has been stable, and that stage at the lower gage, $h_{\text{lower gage}}$, was related to stage at the upper gage, $h_{\text{upper gage}}$, by the following equation

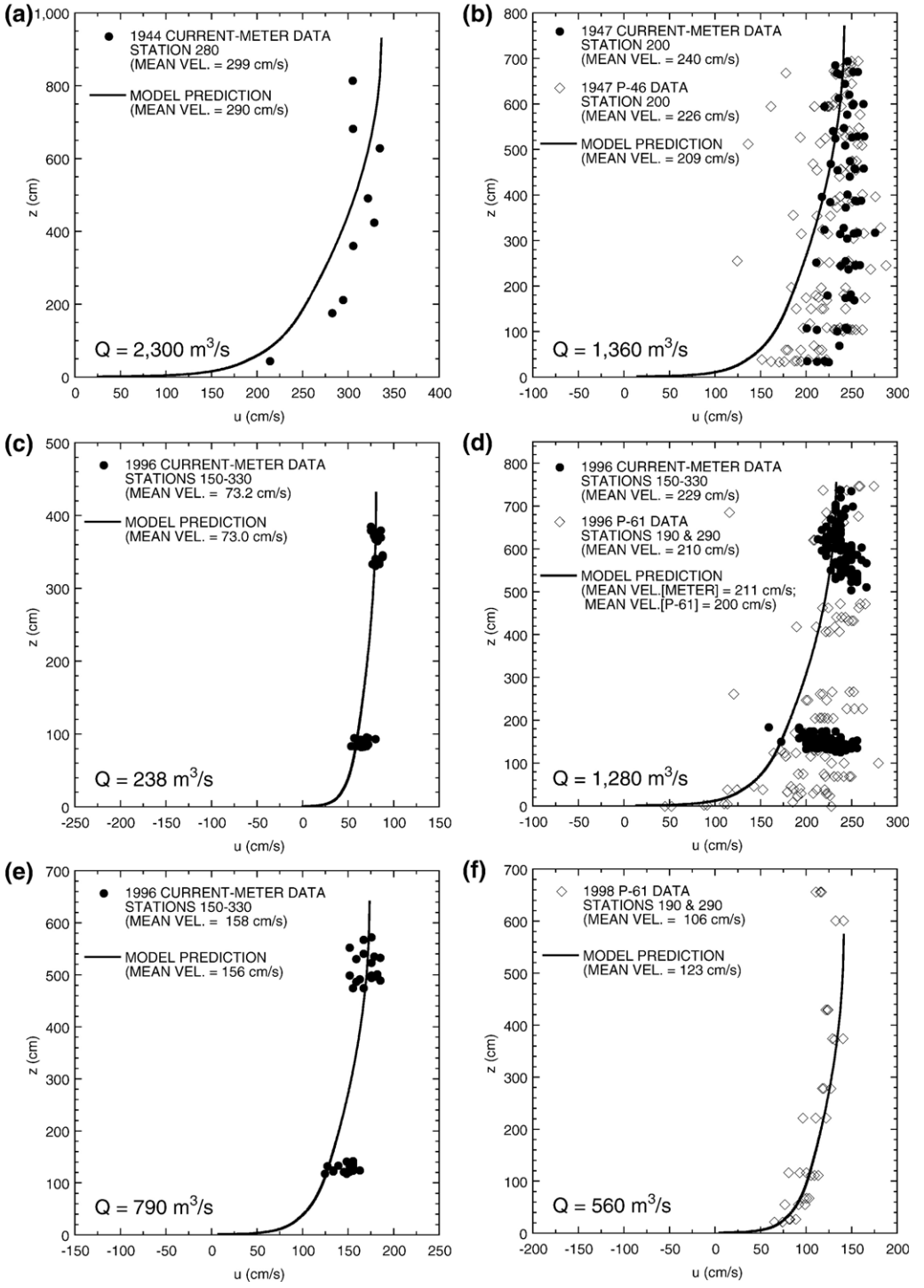

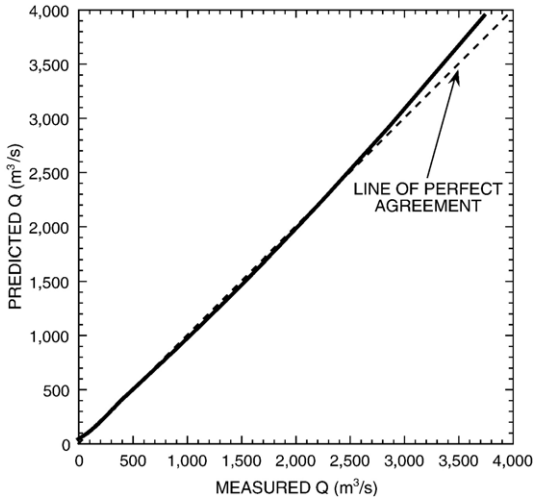

Fig. 8. Model-predicted versus measured water discharge through the cross-section under the measurement cableway at the Grand Canyon gaging station (solid thick line). Measured water discharge was computed from the stage-discharge relation fit to the 3703 pre-dam discharge measurements made by the USGS between November 12, 1922, and March 6, 1963.

determined by linear regression through the data in Fig. 6:

$$h_{\text{lower gage}} = 0.9836(h_{\text{upper gage}}) - 1.8 \quad (15)$$

The R^2 value associated with this equation is 0.9995. Because the upper and lower gages in the reach at the Grand Canyon gaging station are 198 m apart in the streamwise direction and have the same datum, the water-surface slope was calculated as a function of stage from Eq. (14).

If the geometry of the reach at the Grand Canyon gaging station were truly uniform, then the slope of the bed would be equivalent to the water-surface slope, and S_f in Eq. (1) would therefore equal the water-surface slope. Although the cross-section area of the channel decreases in the streamwise direction, because of a lateral recirculation eddy near the upstream end of the reach (Fig. 5), the cross-section area of downstream flow actually increases in the streamwise direction. Thus, the friction slope in this reach is less than water-surface slope. To quantify the friction-slope part of the observed water-surface slope, a step-backwater model was used to estimate the relationship between the water-surface slope and the friction slope. By this approach, the friction slope was found to be related to the water-surface slope by the following equation:

$$S_f = S(0.12 + 0.00058h_{\text{upper gage}}) \quad (16)$$

5.3. Tests of model predictions against data

The predictions from this simple model were tested against a variety of velocity-profile, discharge, and suspended-sediment-concentration data from the pre-dam era in 1944 and 1947, and the post-dam era in 1996 and 1998. The 1947 dataset includes the only point samples of suspended sediment collected in the Colorado River in the pre-dam era. In addition, because the 1947 and 1996 velocity and sediment data were collected at nearly identical discharges, they allow a unique comparison of the vertical structures of velocity and suspended-sand concentration in the pre- and post-dam eras.

The first test of the model was to compare predicted and measured velocity profiles. Model-predicted velocity profiles were therefore compared against velocity-profile data from 1944, 1947, 1996, and 1998 (Fig. 7). This dataset includes velocity profiles that were measured over an order of magnitude range in discharge (i.e., from 238 to 2300 m^3/s). The 1944 data are from Love and Howard (1944), and were measured on May 18, 1944, at a discharge of 2300 m^3/s using a Price current meter at cableway station 280 (Fig. 5). The 1947 data are from

Fig. 9. Model-predicted and measured profiles of suspended-sand concentration and suspended-sand median grain size; also shown are the measured and model-predicted mean concentrations and median grain sizes over the elevation range of the measurements. Model-predicted profiles are computed for A_S=0.38 (the value of the fractional area of the bed covered by fine sediment that provides the best agreement between the model-predicted and measured suspended-sand concentrations among all five cases) and the value of A_S that provides agreement between the model-predicted and measured suspended-sand concentrations in each case; model-predicted profiles of suspended-sand median grain size do not vary as a function of changes in A_S. a Suspended-sand concentration on May 30–June 8, 1947, at cableway station 200, mean Q=1360 m^3/s; agreement between model-predictions and measurements is best when A_S=0.53. b Suspended-sand median grain size on May 30–June 8, 1947. c Suspended-sand concentration on March 28, 1996 at cableway stations 190 and 290, Q=1280 m^3/s; agreement between model-predictions and measurements is best when A_S=0.47. d Suspended-sand median grain size on March 28, 1996. e Suspended-sand concentration on March 30, 1996 at cableway stations 190 and 290, Q=1280 m^3/s; agreement between model-predictions and measurements is best when A_S=0.32. f Suspended-sand median grain size on March 30, 1996. g Suspended-sand concentration on April 2, 1996 at cableway stations 190 and 290, Q=1280 m^3/s; agreement between model-predictions and measurements is best when A_S=0.33. h Suspended-sand median grain size on April 2, 1996. i Suspended-sand concentration on September 26, 1998, at cableway stations 190 and 290, Q=560 m^3/s; agreement between model-predictions and measurements is best when A_S=0.24. j Suspended-sand median grain size on September 26, 1998.

Subcommittee on Sedimentation, Federal Inter-Agency River Basin Committee (1951), and were measured on nine days between May 30 and June 8, 1947, over a discharge range from 1260 to 1440 m^3/s. The mean discharge over the nine days of measurements was 1360 m^3/s; the stage associated with this mean discharge was used as input to the model. These velocity measurements were made at cableway station 200 (Fig. 5) using both a Price current meter and a P-46 point-integrating suspended-sediment sampler. We collected the 1996

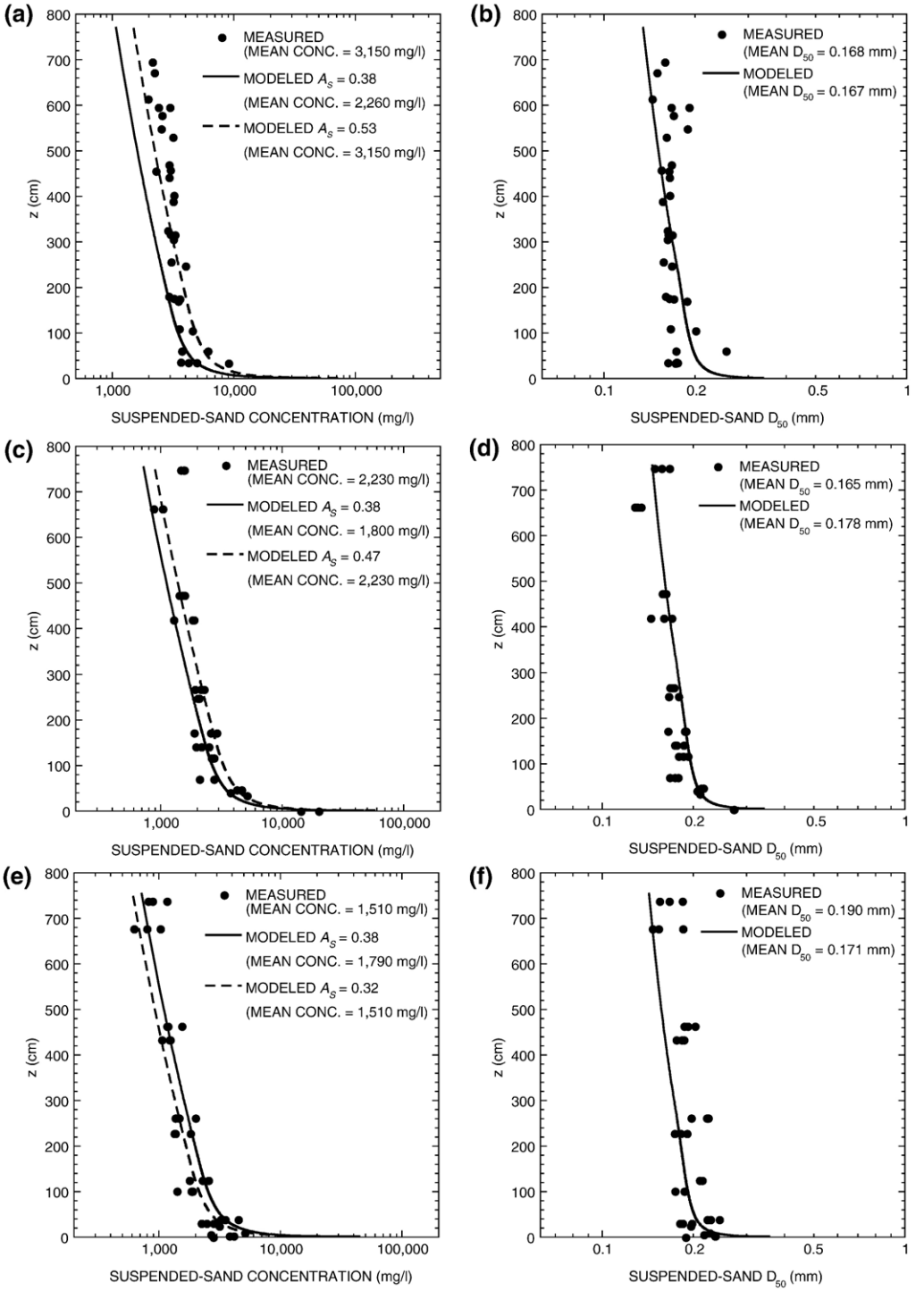

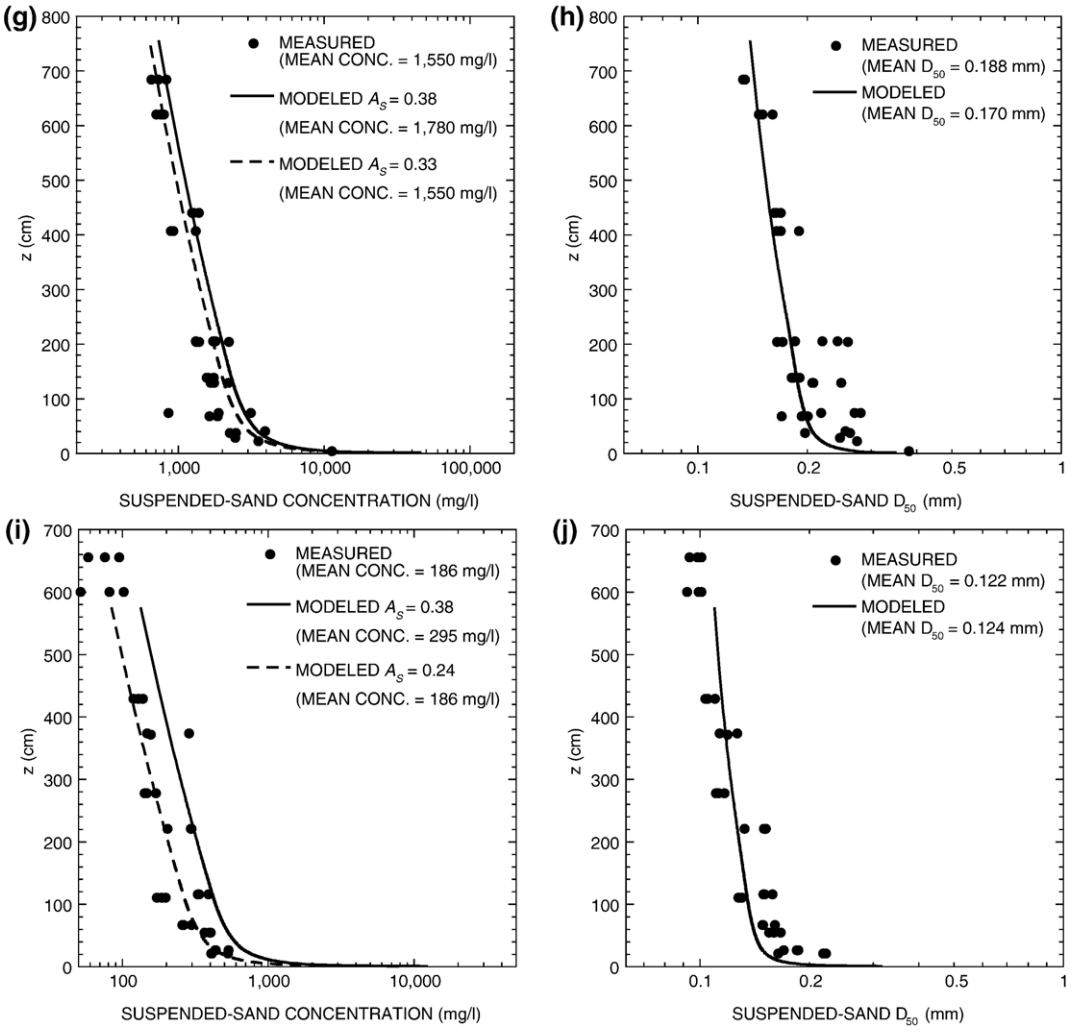

Fig. 9 (*continued*).

velocity data between March 26 and April 3, 1996, at discharges of 238, 1280, and 790 m^3/s using both a Price current meter and a P-61 point-integrating suspended-sediment sampler. The current-meter data were collected at stations spaced every 3.05 m (10 ft) between cableway stations 150 and 330 (Fig. 5). The P-61 velocity data were collected at cableway stations 190 and 290. We collected the 1998 velocity data on September 26, 1998, at a discharge of about 560 m^3/s using a P-61 point-integrating suspended-sediment sampler at cableway stations 190 and 290.

The model does well in predicting the mean velocity over the entire 238 to 2300 m^3/s range in discharge in the 1944–1998 data (mean error is −2.7% and mean absolute value of the error is 14.8%), and does very well in predicting the vertical structure in the velocity profiles measured at a discharge of 2300 m^3/s in 1944, at a discharge of 560 m^3/s in 1998, and at a discharge of 238 m^3/s in 1996. In the discharge range from about 790 to 1360 m^3/s (in the 1947 and 1996 data), however, the model-predicted vertical structure in the velocity profiles tends to be systematically different than that measured, with the modeled near-bed velocities being lower than those measured (Fig. 7). This difference in predicted and measured vertical structure is probably due to that fact that the model was developed using steady, uniform-flow theory and, in reality, the flow in the reach at the Grand Canyon gaging station is nonuniform, with some acceleration occurring at the measurement-cableway cross-section. The higher than predicted near-bed velocities in the profiles measured in the 790–1360 m^3/s discharge range are diagnostic of an accelerating flow. In addition to performing reasonably well in predicting the velocity profiles, the model also does well in reproducing

the average 1922–1963 pre-dam stage-discharge relation (Fig. 8).

The final test of the model was to compare predicted and measured profiles of suspended-sand concentration and grain size (Fig. 9). Model-predicted profiles of suspended-sand concentration and suspended-sand median grain size were therefore compared against suspended-sand-concentration and median-grain-size profile data from 1947, 1996, and 1998. Grain-size distributions of the fine sediment on the bed used as input to the model are shown in Table 1. The $1-\phi$-increment-analyzed 1956 and 1983 grain-size distributions in Table 1 were log-interpolated to $1/2-\phi$ increments along a smoothed curve fit to the $1-\phi$ data prior to being used as input to the model. Model predictions of sand concentration in Fig. 9 were converted from the dimensionless volume fractions used within the model calculations to the more conventional units of mg/l by multiplying by 2,650,000 (this conversion assumes a quartz density of 2.65 g/cm^3 for the sediment). Because bed-sediment grain-size data were not collected during the May 30–June 8, 1947, data-collection period [the first USGS bed-material sampler, the BM-54 (Subcommittee on Sedimentation, Federal Inter-Agency River Basin Committee, 1958) was not available until 1954], the grain-size distribution of the fine sediment on the bed measured on May 31, 1956, was used as input for the model calculations in Fig. 9a,b. This assumption is probably reasonable because the May 30–June 8, 1947, suspended-sediment data and the May 31, 1956, bed sample were collected under similar flow conditions during the annual snowmelt flood, although the May 31, 1956, bed sample was collected immediately prior to the peak of the flood and the 1947 suspended-sediment data were collected during the recession of the flood. Thus, the possibility exists that the 1947 data were collected under slightly more depleted sand-supply conditions than was the May 31, 1956, bed sample. Grain-size distributions of the fine sediment on the bed measured on March 28, 1996, April 2, 1996, and September 26, 1998, were used as input for the model calculations on those days. Because bed-sediment grain-size data were not collected across the middle portion of the cross-section on March 30, 1996, the grain-size distribution of the fine sediment on the bed measured the previous day, March 29, 1996, was used as input for the model calculations in Fig. 9e,f.

The model does well in predicting the mean magnitude (for a fixed value of A_S) and the vertical structure in suspended-sand concentration, and does well in predicting both the mean magnitude and vertical structure in suspended-sand median grain size, for both the pre-dam (1947) data and the post-dam (1996, 1998) data (Fig. 9), although there is a tendency for the depth-averaged gradients in some of the model-predicted concentration profiles to be less than those measured (Fig. 9a,c). As previously observed in the cases of the velocity profiles measured in the discharge range from about 790 to 1360 m^3/s, this result is also typical in a slightly accelerating flow. The mean error between the model-predicted median grain size and the measured median grain size of the suspended sand among the five cases is −2.1%; the mean absolute value of the error between the model-predicted median grain size and the measured median grain size of the suspended sand among the five cases is 5.9%. Note that changes in A_S affect only the mean suspended-sand concentration, not the vertical structure in suspended-sand concentration, the mean suspended-sand median grain size, nor the vertical structure in suspended-sand median grain size.

The best agreement between the model-predictions and measurements of suspended-sand concentration for all cases occurs with a value of A_S equal to about 0.38. If this value is held constant, the model underpredicts suspended-sand concentration by 28% relative to the 1947 measurements, underpredicts suspended-sand concentration by 19% relative to the March 28, 1996, measurements, overpredicts suspended-sand concentration by 19% relative to the March 30, 1996, measurements, overpredicts suspended-sand concentration by 15% relative to the April 2, 1996, measurements, and overpredicts suspended-sand concentration by 58% relative to the September 26, 1998, measurements. Thus, the mean error introduced into the model-predicted suspended-sand concentrations by holding A_S constant is +9.0%; the mean absolute value of the error introduced into the model-predicted suspended-sand concentrations by holding A_S constant is 28%.

If A_S is allowed to vary, the best agreement between the model-predictions and measurements of suspended-sand concentration occur with values of A_S of 0.53 for the pre-dam (1947) data, and ranging from 0.24 to 0.47 for the post-dam (1996–1998) data. The post-dam model-predicted values of A_S are reasonable compared to the 20 to 40% values for the area of bed-sand coverage measured using side-scan sonar in 1994, 1996, 1998, 1999, and 2000 (Anima et al., 1998; Wong et al., 2003; S. Goeking, Utah State University, unpublished 2004 analysis of 2000 data of R. Anima; R. Anima, written communication, 2006). For the September 26, 1998, data, the best agreement between the model-predictions and measurements of suspended-sand concentration occurs when A_S is equal to 0.24. Side-scan-sonar mapping of bed texture conducted on September 25–26, 1998 indicates that, on these days, approximately 33% of the

Table 1
Cross-sectionally averaged median grain sizes and cumulative grain-size distributions of the fine sediment on the bed under the measurement cableway at the Grand Canyon gaging station [a]

Date	Fine-sed.	Mean cumulative grain-size distribution of fine sediment on bed (% finer than)										
	D_{50} (mm)	0.063 (mm)	0.088 (mm)	0.125 (mm)	0.177 (mm)	0.250 (mm)	0.354 (mm)	0.500 (mm)	0.707 (mm)	1.00 (mm)	1.41 (mm)	2.00 (mm)
4-12-1956	0.20	0.0		5.0		61.0		99.0		100.0		100.0
5-31-1956	0.40	0.0		1.0		12.1		80.8		99.0		100.0
6-25-1983	0.71	0.0		0.1		1.9		26.1		77.9		100.0
10-3-1983	0.33	0.8		5.9		27.7		90.6		99.3		100.0
3-27-1996	0.32	0.1	0.6	2.6	8.4	25.6	59.2	93.3	99.3	99.8	100.0	100.0
3-28-1996	0.39	0.1	0.2	0.7	2.8	11.2	36.7	82.7	97.6	99.5	99.8	100.0
3-29-1996	0.41	0.1	0.2	0.8	2.8	10.9	32.0	75.5	95.5	99.0	99.8	100.0
4-1-1996	0.42	0.0	0.1	0.6	2.0	7.7	27.2	70.7	90.5	95.4	98.0	100.0
4-2-1996	0.40	0.0	0.1	0.8	2.8	10.2	34.5	81.5	96.0	98.8	99.6	100.0
9-26-1998	0.41	0.1	0.3	1.3	4.5	12.8	33.4	75.3	91.6	96.5	98.6	100.0
11-22-2004	0.31	0.5	1.6	4.8	12.8	29.3	61.4	90.2	97.2	98.6	99.4	100.0
11-24-2004	0.41	0.1	0.3	1.4	4.4	12.0	34.0	67.6	84.3	92.3	96.7	100.0

[a] Grain-size distributions determined by dry sieving. 1956 data are from Love (1961), 1983 data from Garrett et al. (1993), 1996 data from Topping et al. (1999), and 2004 data from www.gcmrc.gov. Dates are shown in month-day-year.

bed was covered by sand in the 2.6-km-long reach upstream from the measurement cableway, with the sand coverage increasing from <16% at the head of this reach to 24% 1.4 km upstream from the cableway, then rapidly increasing to about 54% under the cableway (R. Anima, written communication, 2006). Therefore, the model-predicted value of A_S=24% and the observed fractional area of fine sediment on the bed, increasing from 16% upstream to 54% downstream, are in reasonable agreement for the September 1998 case. The pre-dam model-predicted value of A_S is also reasonable in that Glen Canyon Dam has reduced the supply of sand to the Colorado River in the reach at the Grand Canyon gaging station by about 85 to 90% (Topping et al., 2000a; Wright et al., 2005). However, it is important to note that the only existing pre-dam suspended-sand-profile data were collected during the recession of the annual snowmelt flood in 1947, during a period when the pre-dam Colorado River would be relatively depleted with respect to sand (Topping et al., 2000a). Therefore, it is likely that the pre-dam value of the area of bed-sand coverage was greater than 50% during the nine months of the year when the discharge of water was typically less than 250 m^3/s, and sand accumulated in the reach between the Lees Ferry and Grand Canyon gaging stations (Topping et al., 2000a). Because the model performed very well in predicting velocity, water discharge, suspended-sand concentration, and suspended-sand grain size in these test cases, the final step in this study was to use the model to evaluate the importance of changes in (1) the grain-size distribution of the fine-sediment on the bed and (2) the fractional area of the bed that is covered by fine sediment over a wider range of pre-dam and post-dam sand-supply conditions.

5.4. Application of the model to the entire range of pre- and post-dam sand-supply conditions

To determine the relative importance of changes in the grain size of fine sediment on the bed and changes in the area of the bed covered by fine sediment, the model was used to construct suspended-sand-concentration and grain-size rating curves associated with the pre- and post-dam cases where the grain-size distribution of the fine sediment on the bed was measured (Figs. 10 and 11). To illustrate the effects of varying A_S on model-predicted suspended-sand concentration, suspended-sand-concentration rating

Fig. 10. Model-predicted rating curves relating suspended-sand concentration to the discharge of water for measured grain-size distributions of the fine sediment on the bed. Rating curves are computed for values of A_S equal to 1.0, 0.5, and 0.25. Also shown are the pre- and post-dam measurements of cross-sectionally averaged suspended-sand concentration; indicated are the measured suspended-sand concentrations that correspond to the measured "fine bed" or "coarse bed" case. In this figure and Fig. 11, pre-dam data (n=616) were collected between July 26, 1944, and March 4, 1963; post-dam data (n=1965) were collected between September 8, 1965, and November 30, 2004. a Curves computed for the April 12, 1956, fine-bed case and the May 31, 1956, coarse-bed case. b Curves computed for the June 25, 1983 coarse-bed case and the October 3, 1983, fine-bed case. c Curves computed for the March 27, 1996, fine-bed case and the April 1, 1996, coarse-bed case. d Curves computed for the November 22, 2004, fine-bed case and the November 24, 2004, coarse-bed case.

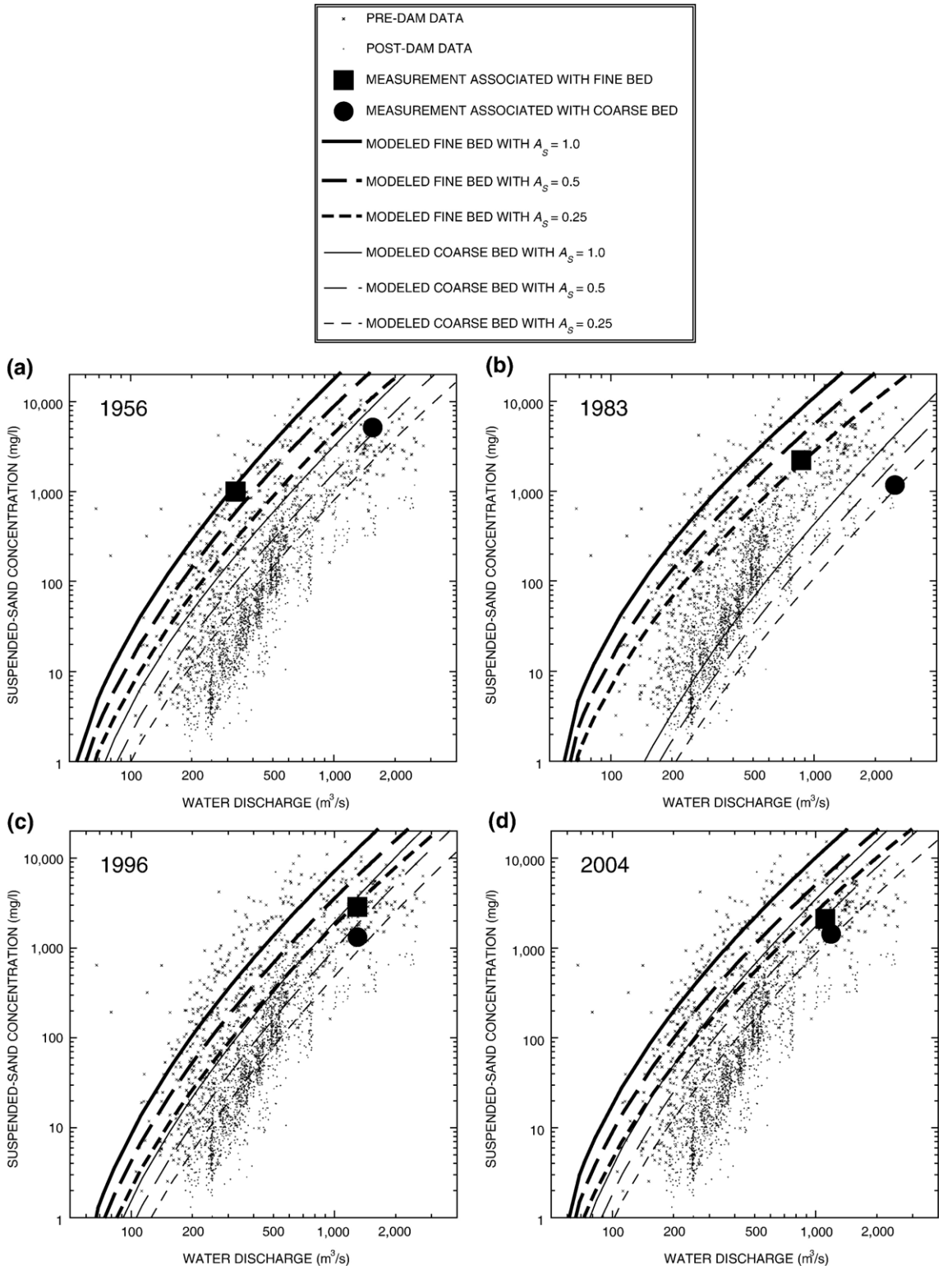
PRE-DAM DATA
POST-DAM DATA
MEASUREMENT ASSOCIATED WITH FINE BED
MEASUREMENT ASSOCIATED WITH COARSE BED
MODELED FINE BED WITH A_S = 1.0
MODELED FINE BED WITH A_S = 0.5
MODELED FINE BED WITH A_S = 0.25
MODELED COARSE BED WITH A_S = 1.0
MODELED COARSE BED WITH A_S = 0.5
MODELED COARSE BED WITH A_S = 0.25
(a)
1956
(b)
1983
(c)
1996
(d)
2004
SUSPENDED-SAND CONCENTRATION (mg/l)
WATER DISCHARGE (m3/s)
10,000
1,000
100
10
1
100
200
500
1,000
2,000

curves were calculated for different values of A_S. The grain-size distributions of the fine-sediment on the bed used as input to the model are presented in Table 1.

The pre-dam cases to which the model was applied were the fine-bed condition (D_{50}=0.20 mm) measured on April 12, 1956, and the coarse-bed condition (D_{50}=0.40 mm) measured on May 31, 1956 (Fig. 5a in Topping et al., 2000a). These two cases are the only two pre-dam days on which the grain-size distribution of the fine sediment on the bed was measured at the Grand Canyon gaging station. The April 12, 1956, fine-bed measurement was made following the nine-month season of sand accumulation upstream from the Grand Canyon gaging station and prior to the 1900 m^3/s peak discharge of the 1956 snowmelt flood on June 2. The discharge of water at the time of this measurement was about 330 m^3/s. The May 31, 1956 coarse-bed measurement was made during the final part of the rising limb of the 1956 snowmelt flood. The discharge of water at the time of this measurement was about 1070 m^3/s.

The post-dam cases to which the model was applied were the coarse-bed condition (D_{50}=0.70 mm) measured on June 25, 1983, the fine-bed condition (D_{50}=0.30 mm) measured on October 2, 1983, the fine-bed condition (D_{50}=0.32 mm) measured on March 27, 1996, the coarse-bed condition (D_{50}=0.42 mm) measured on April 1, 1996, the fine-bed condition (D_{50}=0.31 mm) measured on November 22, 2004, and the coarse-bed condition (D_{50}=0.41 mm) measured on November 24, 2004. The June 25, 1983, coarse-bed measurement was made during the final part of the rising limb of the 1983 flood, the largest flood released from Glen Canyon Dam. The peak discharge of this flood was 2750 m^3/s, and the discharge of water at the time of this measurement was about 1960 m^3/s. Suspended-sediment measurements were not made during the 1983 flood until July 1, however. Therefore, the suspended-sand concentration and median grain size modeled using the June 25, 1983, bed data as input were compared with the July 1, 1983, suspended-sand data. The October 3, 1983, fine-bed measurement was made immediately following a 300 m^3/s flood on the Little Colorado River, which enters the Colorado River 41 km upstream from the Grand Canyon gaging station (Fig. 1). This tributary flood supplied about one million metric tons of fine and very fine sand to the Colorado River, resulting in substantial fining of the channel bed (Topping et al., 2000b). The March 27, 1996 fine-bed measurement was made during the first day of a seven-day experimental artificial flood (the 1996 controlled flood) released from Glen Canyon Dam. Substantial coarsening of the fine sediment on the bed occurred during this flood in response to the depletion of the upstream supply of finer sand (Rubin et al., 1998; Topping et al., 1999, 2000b). The April 1, 1996, coarse-bed measurement was made on day six of this flood. The November 22, 2004, fine-bed measurement was made during the final part of the rising limb of a 60-hour experimental artificial flood (the 2004 controlled flood) released from Glen Canyon Dam. Substantial coarsening of the fine sediment on the bed occurred also during this flood in response to the depletion of the upstream supply of finer sand (Topping et al., 2006a). The November 24, 2004, coarse-bed measurement was made during the last day of high discharge during this flood.

The suspended-sand concentration rating curves in Fig. 10 allow separation of the effects on suspended-sand concentration of changing water discharge, changing grain size of the fine sediment on the bed, and changing fractional area of the fine sediment on the bed. This application of the model to a wider range of pre- and post-dam conditions than those in the preceding section indicates that considerable error is introduced into the model predictions of suspended-sand concentration by holding A_S constant at 0.38 (Table 2), although this error is still much smaller than the one to two order of magnitude error that would be introduced into the model predictions of suspended-sand concentration by ignoring the effects of changes in the grain size of the fine sediment on the bed. To more fully explore the likely importance of changes in the fractional area of fine sediment on the bed, the model was used to predict the values of A_S that result in bringing the model-predicted suspended-sand concentrations into perfect agreement with the measured suspended-sand concentrations (Table 2). The results presented in Fig. 10 and Table 2 indicate that the observed changes in bed-sediment grain size are responsible for well over an order of magnitude change in suspended-sand concentration (determined from comparison of the 1983 rating curves in Fig. 10b), and that the maximum change in suspended-sand concentration that could be attributed to changes in the fractional area of fine sediment on the bed is about 60% (during the 2004 controlled flood). The factor of 30 increase in suspended-sand concentration caused by the factor of two fining of the fine sediment on the bed after the 1983 Little Colorado River flood was accompanied by only a 3.6% model-predicted change in A_S (i.e., no real demonstrable change in A_S). Likewise, the factor of two coarsening of the fine sediment on the bed during the 1956 snowmelt flood resulted in a factor of six decrease in suspended-sand concentration, whereas changes in A_S of a factor of two (i.e., about the largest required to force perfect agreement between the model predictions and the data) will only result in a factor of two change in suspended-sand concentration.

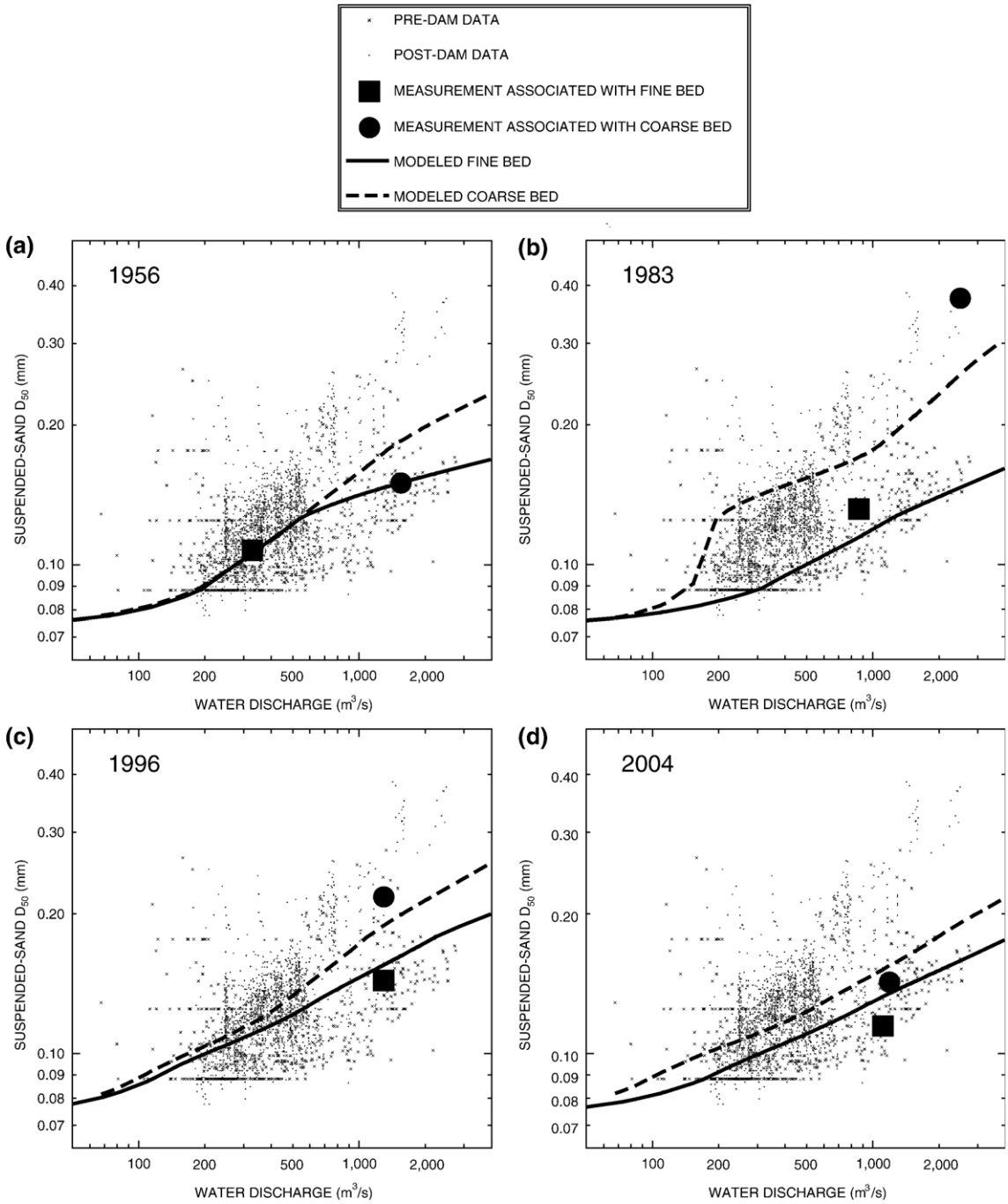

Fig. 11. Model-predicted rating curves relating suspended-sand median grain size to the discharge of water for measured grain-size distributions of the fine sediment on the bed. Also shown are the pre- and post-dam measurements of cross-sectionally averaged suspended-sand median grain size; indicated are the measured suspended-sand median grain sizes that correspond to the measured "fine bed" or "coarse bed" case. a Curves computed for the April 12, 1956, fine-bed case and the May 31, 1956, coarse-bed case. b Curves computed for the June 25, 1983, coarse-bed case and the October 3, 1983, fine-bed case. c Curves computed for the March 27, 1996, fine-bed case and the April 1, 1996, coarse-bed case. d Curves computed for the November 22, 2004, fine-bed case and the November 24, 2004, coarse-bed case.

Table 2
Calculated values of the percent error between the model-predicted and measured cross-sectionally averaged suspended-sand concentrations introduced by holding A_S constant at 0.38, the fractional area of the fine sediment on the bed, A_S, that results in bringing the model-predicted cross-sectionally averaged suspended-sand concentrations into perfect agreement with the measured cross-sectionally averaged suspended-sand concentrations, and the percent error between the model-predicted and measured cross-sectionally averaged median grain size (D_{50}) of the suspended sand

	Error in model-predicted suspended-sand concentration introduced by A_S=0.38 (%)	A_S for perfect agreement between model-predicted and measured suspended-sand concentrations	Error in model-predicted median grain size of the suspended sand (%)
1956 fine-bed case; April 12	−59.1	0.93	−2.7
1956 coarse-bed case; May 31	−37.7	0.61	+21.3
1983 coarse-bed case; June 25	+26.3	0.28	−32.8
1983 fine-bed case; October 3	+31.0	0.29	+14.2
1996 fine-bed case; March 27	+52.0	0.25	+6.7
1996 coarse-bed case; April 1	+2.7	0.37	−14.3
2004 fine-bed case; November 22	+111.1	0.18	+13.9
2004 coarse-bed case; November 24	+31.0	0.29	−7.0
Mean results	−48.8 pre-dam, +42.4 post-dam	0.77 pre-dam, 0.28 post-dam	−0.1

Although the lowest concentrations of suspended sand measured at the Grand Canyon gaging station could be modeled using extremely low values of A_S (<1%) and by holding the grain size of the fine sediment on the bed constant at a typical value, this result is not supported by the available observations of areal coverage of fine sediment on the bed and conflicts with observations of suspended-sand grain size. If the fractional area of the fine sediment on the bed ever decreased to such low values, it would have done so during the period following the 2750 m^3/s flood released from Glen Canyon Dam in 1983. Sand depletion during the 1983 flood resulted in the coarsest grain-size distributions of fine sediment ever measured on the bed at the Grand Canyon gaging station (Fig. 4 in Topping et al., 2005). Side-scan-sonar data collected between the Lees Ferry and Grand Canyon gaging stations during March 1984 (Wilson, 1986) indicated that dunes on sand patches comprised about 11% of the bed, and "smooth bottom" (composed of a mixture of sand and gravel) comprised about 38% of the bed (Randle and Pemberton, 1987). Thus, the minimum observed value of A_S exceeded 11% and was more likely 20% during the period of greatest sand depletion (i.e., the period following the 1983 flood). Finally, use in the model of extremely low values of A_S and a constant typical grain size of the fine sediment on the bed would result in predicted median grain sizes of the suspended sand that do not track with the observed changes in the median grain size of the suspended sand (shown below).

Despite the simplification of real physical sediment-entrainment processes that is inherent in the lower boundary condition for suspended sediment, the model-predicted value of A_S is in reasonable agreement with the observed fractional area of fine sediment on the bed for the only case in which suspended-sediment and bed-textural data were collected at the same time (during September 25–26, 1998). Furthermore, the changes in A_S are in agreement with the changes in the fractional area of fine sediment on the bed reported in previous geomorphic studies (Anima et al., 1998; Topping et al., 2000a; Schmidt et al., 2004). The model results suggest that, although they were not the dominant regulator of suspended-sand concentration, substantial systematic changes in the fractional area of the fine sediment on the bed occurred during both pre- and post-dam Colorado River floods (but in different directions). During the 1956 snowmelt flood, the model results indicate that A_S decreased by 34% (from 0.93 to 0.61). This result is consistent with the observation that during the average annual snowmelt flood, between 1.7 and 13 million metric tons of sand were eroded from storage in the reach upstream from the Grand Canyon gaging station (Topping et al., 2000a). To place these numbers in perspective, erosion of 13 million metric tons of sand is equivalent to about 60 cm of erosion everywhere on the bed of the river in the 141-km-long reach between the Lees Ferry and Grand Canyon gaging stations. In other words, this magnitude of seasonal erosion was large enough that it must have resulted in a decrease in the fractional area of the fine sediment on the bed. In contrast to this pre-dam case, the model results indicate that A_S increased during two post-dam floods; A_S increased by 48% during the 1996 controlled flood (from 0.25 to 0.37) and by 61% during the 2004 controlled flood (from 0.18 to 0.29). The model-predicted increase in A_S

during these two controlled floods is consistent with the results from side-scan-sonar mapping of bed texture conducted before and after short-duration, high dam releases. These side-scan-sonar results indicate that, in reaches upstream from the Grand Canyon gaging station, the fractional area of fine sediment on the bed increased during the 1996 controlled flood (Anima et al., 1998) and during a second high dam release in September 2000 (S. Goeking, Utah State University, unpublished 2004 analysis of 2000 data of R. Anima). Finally, the model results indicate that the 1963 closure and operation of Glen Canyon Dam has resulted in an approximate 64% average decrease in A_S (from 0.77 to 0.28). This result is consistent with the results of every geomorphic study conducted in the reach between Glen Canyon Dam and the Grand Canyon gaging station. These studies have shown that about 20 million metric tons of sand were eroded from this reach in 1965 alone (this amount of erosion is equivalent to about 90 cm of erosion everywhere in the 165-km-long reach between the dam and the Grand Canyon gaging station) and that substantial erosion of sandbars continues; results from these numerous studies are summarized in Rubin et al. (2002), Schmidt et al. (2004), and Wright et al. (2005). Although we have only one independent quantitative measurement with which to test the model-predicted value of A_S (on September 25–26, 1998), all model-predicted values of A_S are consistent with the qualitative observations cited above.

The suspended-sand median-grain-size rating curves in Fig. 11 allow separation of the effects on suspended-sand grain size of changing water discharge and changing grain size of the fine sediment on the bed. By virtue of the physics in the model, the grain size of the sand in suspension does not depend on the fractional area of the fine sediment on the bed. Disagreement (in percent) between the model-predicted median size of the suspended sand and the measured median size of the suspended sand for each case is presented in Table 2. The mean disagreement between the model predictions and measurements of the median size of the suspended sand is −0.1% for all eight cases, with the largest disagreement being −32.8% during 1983. Even a disagreement of 33% between model predictions and measurements of the median grain size of suspended sand is, however, quite small. Because the agreement was good between the model-predicted and measured profiles of the median grain size of the suspended sand in the central part of the channel (Fig. 9), disagreement between the model predictions and measurements of the cross-sectionally averaged median grain size of the suspended sand can be best explained in two ways. First, the limited number of bed-sediment samples collected under the measurement cableway may be insufficient to accurately characterize the average grain-size composition of the bed upstream from the cableway. To alleviate this problem of sparse data, Chezar (2001), Rubin (2004), Rubin et al. (2007-this volume) have developed an approach using a digital underwater microscope that can be used to rapidly collect a more representative, spatially robust dataset of the grain size of the fine sediment on the bed. Second, the mean error in cross-sectionally averaged measurements of the median grain size of suspended sand measured made using depth-integrating suspended-sediment samplers has been found to exceed 10% at the Grand Canyon gaging station (Topping et al., 2006b). Grain-size errors between paired individual samples can be much larger. For example, on April 1, 1996, the cross-sectionally averaged median grain size of the suspended sand measured with a P-61 point-integrating suspended-sediment sampler operated in the depth-integrating mode was 0.217 mm (the value against which the model prediction of 0.186 mm was compared), whereas the cross-sectionally averaged median grain size of the suspended sand measured with a D-77 depth-integrating suspended-sediment bag sampler was 0.178 mm. The errors between these paired samples are approximately 20%. Only slight contamination of a suspended-sediment sample with bed sand (when the sampler nozzle hits the bed) can result in errors larger than 100% (Allen and Petersen, 1981).

6. Conclusions

Grain size of the fine sediment on the bed is the dominant regulator of suspended-sand concentration in the Colorado River at the Grand Canyon gaging station during both the pre- and post-dam eras. In contrast, changes in the fractional area of the bed that is covered by fine sediment play only a minor role in regulating suspended-sand concentration. This result is consistent with existing sediment-transport theory and experiments, which show that the dependence of suspended-sand concentration on bed-sand grain size is highly nonlinear (e.g., Engelund and Hansen, 1967; Rubin and Topping, 2001) and the spatially averaged dependence of suspended-sand concentration on the area of the bed covered by sand is quasi-linear (Topping, 1997; Grams, 2006).

Because the dominant coupling between suspended-sand concentration and the sand on the bed of the river is through the grain size of the sand on the bed, and not the area or amount of sand on the bed, abrupt changes in the upstream supply of sand will result in rapid and large

changes in bed-sand grain size, and relatively small changes in the area of bed sand. In certain cases, decreases in the upstream supply of sand may actually be associated with increases in the area of the sand on the bed (e.g., during the 1996 and 2004 controlled floods). Thus, changes in bed-sand grain size may override the effects of changes in bed-sand area in regulating suspended-sand concentration. Changes in the area of sand on the bed do not result in changes in the grain size of the sand in suspension. Therefore, as shown in Rubin et al. (1998), grain-size trends in fluvial deposits produced during floods are controlled by changes in the grain size of the sand in suspension, which are in turn controlled by changes in the grain size of the sand on the bed driven by changes in the upstream sand supply. These changes in the grain size of the sand supplied to depositional sites may alone cause changes in the configuration of the bedforms preserved in deposits, with no required change in either the discharge of water (Rubin et al., 1998) or the area of sand on the bed.

Acknowledgments

Funding for this research was provided by the U.S. Department of the Interior's Glen Canyon Dam Adaptive Management Program through the USGS Grand Canyon Monitoring and Research Center. We thank Roberto Anima for generously supplying the unpublished results from his side-scan-sonar mapping programs. Reviews by Jon Warrick, Giles Lesser, and an anonymous reviewer greatly improved the quality of this paper.

References

Allen, P.B., Petersen, D.V., 1981. A study of the variability of suspended sediment measurements: Erosion and Sediment Transport Measurements. Proceedings of the Florence Symposium, June 1981. IAHS pub., vol. 133, pp. 203–211.

Anima, R.J., Marlow, M.S., Rubin, D.M., Hogg, D.J., 1998. Comparison of sand distribution between April 1994 and June 1996 along six reaches of the Colorado River in Grand Canyon, Arizona. U.S. Geological Survey Open-File Report, pp. 98–141.

Best, J., 2005. The fluid mechanics of river dunes: a review and some future research directions. Journal of Geophysical Research 110, F04S02 21 pp.

Chezar, H., 2001. Underwater microscope system. U.S. Geological Survey Fact Sheet, p. 135-01.

Dietrich, W.E., 1982. Settling velocity of natural particles. Water Resources Research 18, 1615–1626.

Edwards, T.K., Glysson, G.D., 1999. Field methods for measurement of fluvial sediment. Techniques of Water-Resources Investigations of the U.S. Geological Survey, Book 3, Chapter C2.

Einstein, H.A., Chien, N., 1953. Transport of sediment mixtures with large ranges of grain size. University of California, Berkeley, CA, Missouri River District Sediment Series, vol. 2.

Engelund, F., Hansen, E., 1967. A Monograph on Sediment Transport in Alluvial Streams, 2nd edition. Teknisk Forlag, Copenhagen, Denmark.

Federal Interagency Sedimentation Project, 2001. The US D-96: an isokinetic suspended-sediment/water-quality collapsible-bag sampler. Waterways Experiment Station, Vicksburg, MS, Report PP.

Federal Interagency Sedimentation Project, 2003. The US D-96: an isokinetic suspended-sediment/water-quality collapsible-bag sampler. The US D-96-A1: a lightweight version of the US D-96. Waterways Experiment Station, Vicksburg, MS. Report PP Addendum-II.

Garrett, W.B., Van De Vanter, E.K., Graf, J.B., 1993. Streamflow and sediment-transport data, Colorado River and three tributaries in Grand Canyon, Arizona, 1983 and 1985–86. U.S. Geological Survey Open-File Report, pp. 93–174.

Gelfenbaum, G., Smith, J.D., 1986. Experimental evaluation of a generalized suspended-sediment transport theory. In: Knight, R.J., McLean, J.R. (Eds.), Shelf sands and sandstones. Canadian Society of Petroleum Geologists Memoir, vol. II, pp. 133–144.

Grams, P.E., 2006. Sand transport over a coarse and immobile bed. PhD Thesis, The Johns Hopkins University, Baltimore, MD (http://www.gcmrc.gov/library/reports/physical/Fine_Sed/Grams2006.pdf).

Guy, H.P., Simons, D.B., Richardson, E.V., 1966. Summary of alluvial channel data from flume experiments, 1956–61. U.S. Geological Survey Professional Paper 462-I.

Hunt, J.N., 1969. On the turbulent transport of a heterogeneous sediment. The Quarterly Journal of Mechanics and Applied Mathematics 22, 235–246.

Kennedy, J.F., 1961. Stationary waves and antidunes in alluvial channels. California Institute of Technology, Division of Engineering, Pasadena, CA, W.M. Keck Laboratory of Hydraulics and Water Resources Report No. KH-R-2.

Long, C.E., Wiberg, P.L., Nowell, A.R.M., 1993. Evaluation of von Karman's constant from integral flow parameters. Journal of Hydraulic Engineering 119, 1182–1190.

Love, S.K., 1961. Quality of surface waters of the United States 1957. Parts 9–14. Colorado River basin to Pacific slope basins in Oregon and lower Columbia River basin. U.S. Geological Survey Water-Supply Paper, vol. 1523.

Love, S.K., Howard, C.S., 1944. Appendix A. Field tests of the US D-43 sediment sampler in the Colorado River Basin, May 1944. In: Subcommittee on Sedimentation, Federal Inter-Agency River Basin Committee (Eds.), Progress report. Comparative field tests on suspended sediment samplers: a study of methods used in measurement and analysis of sediment loads in streams. Report C. University of Iowa Hydraulic Laboratory, Iowa City, IA.

McLean, S.R., 1991. Depth-integrated suspended-load calculations. Journal of Hydraulic Engineering 117, 1440–1458.

McLean, S.R., 1992. On the calculation of suspended load for noncohesive sediments. Journal of Geophysical Research 97, 5759–5770.

Middleton, G.V., Southard, J.B., 1984. Mechanics of sediment movement. Tulsa, OK, SEPM Short Course Number 3.

Monin, A.S., Yaglom, A.M., 1965. Statisicheskaya gidromekhanika — Mekhanika turbulentnosti. Nauka Press, Moscow (English translation by Scripta Technica, Inc., 1971, Statistical fluid mechanics: mechanics of turbulence, v. 1. MIT Press, Cambridge, MA).

Nelson, J.M., McLean, S.R., Wolfe, S.R., 1993. Mean flow and turbulence fields over 2-dimensional bed forms. Water Resources Research 29, 3935–3953.

Nordin Jr., C.F., 1963. A preliminary study of sediment transport parameters, Rio Puerco near Bernardo, New Mexico. U.S. Geological Survey Professional Paper 462-C.

Parker, G., 1978. Self-formed straight rivers with equilibrium banks and mobile bed. Part 1. The sand-silt river. Journal of Fluid Mechanics 89, 109–125.

Randle, T.J., Pemberton, E.L., 1987. Results and analysis of STARS modeling efforts of the Colorado River in Grand Canyon. National Technical Information Service Report GCES/11/87 (http://www.gcmrc.gov/library/reports/physical/Fine_Sed/Randle1987.pdf).

Rattray Jr., M., Mitsuda, E., 1974. Theoretical analysis of conditions in a salt wedge. Estuarine Coastal Marine Science 2, 373–394.

Rouse, H., 1937. Modern conceptions of the mechanics of turbulence. Transactions of the American Society of Civil Engineers 102, 463–543.

Rubin, D.M., 2004. A simple autocorrelation algorithm for determining grain size from digital images of sediment. Journal of Sedimentary Research 74, 160-105.

Rubin, D.M., Topping, D.J., 2001. Quantifying the relative importance of flow regulation and grain-size regulation of suspended-sediment transport (α), and tracking changes in bed-sediment grain size (β). Water Resources Research 37, 133–146.

Rubin, D.M., Nelson, J.M., Topping, D.J., 1998. Relation of inversely graded deposits to suspended-sediment grain-size evolution during the 1996 Flood Experiment in Grand Canyon. Geology 26, 99–102.

Rubin, D.M., Topping, G.M., Anima, D.J., 2001. Use of rotating side-scan sonar to measure bedload. Proceedings of the 7th Inter-Agency Sedimentation Conference, vol. 1, pp. III/139–III/143. Reno, NV, March 25–29.

Rubin, D.M., Topping, D.J., Schmidt, J.C., Hazel, J., Kaplinski, K., Melis, T.S., 2002. Recent sediment studies refute Glen Canyon Dam hypothesis. EOS Transactions American Geophysical Union 83(25), 273, 277–278.

Rubin, D.M., Chezar, H., Harney, J.N., Topping, D.J., Melis, T.S., Sherwood, C.R., 2007. Underwater microscope for measuring spatial and temporal changes in bed-sediment grain size. Sedimentary Geology 202, 402–408 (this volume), doi:10.1016/j.sedgeo.2007.03.020.

Schmidt, J.C., Topping, D.J., Grams, P.E., Hazel, J.E., 2004. System-wide changes in the distribution of fine sediment in the Colorado River corridor between Glen Canyon Dam and Bright Angel Creek, Arizona. Final report to the USGS Grand Canyon Monitoring and Research Center, Flagstaff, AZ. http://www.gcmrc.gov/library/reports/physical/Fine_Sed/Schmidt2004.pdf.

Smith, J.D., 1977. Modeling of sediment transport on continental shelves. In: Goldberg, E.D. (Ed.), The Sea, vol. 6. Wiley, New York, pp. 539–577.

Smith, J.D., McLean, S.R., 1977. Spatially averaged flow over a wavy surface. Journal of Geophysical Research (Oceans) 82, 1735–1746.

Subcommittee on Sedimentation, Federal Inter-Agency River Basin Committee, 1951. Progress report. Field tests on suspended sediment samplers, Colorado River at Bright Angel Creek near Grand Canyon, Arizona: a study of methods used in measurement and analysis of sediment loads in streams. Report F. St. Anthony Falls Hydraulic Laboratory, Minneapolis, MN.

Subcommittee on Sedimentation, Federal Inter-Agency River Basin Committee, 1958. Operation and maintenance of US BM-54 bed-material sampler: a study of methods used in measurement and analysis of sediment loads in streams. Report M. St. Anthony Falls Hydraulic Laboratory, Minneapolis, MN.

Tennekes, H., Lumley, J.L., 1972. A first course in turbulence. MIT Press, Cambridge, MA.

Topping, D.J., 1997. Physics of flow, sediment transport, hydraulic geometry, and channel geomorphic adjustment during flash floods in an ephemeral river, the Paria River, Utah and Arizona. PhD Thesis, University of Washington, Seattle, WA (2 volumes, http://www.gcmrc.gov/library/reports/physical/Fine_Sed/Topping1997V1.pdf, and http://www.gcmrc.gov/library/reports/physical/Fine_Sed/Topping1997V2.pdf).

Topping, D.J., Rubin, D.M., Nelson, J.M., Kinzel III, P.J., Bennett, J.P., 1999. Linkage between grain-size evolution and sediment depletion during Colorado River floods. In: Webb, R.H., Schmidt, J.C., Marzolf, G.R., Valdez, R.A. (Eds.), The 1996 Controlled Flood in Grand Canyon. Geophysical Monograph, vol. 110. American Geophysical Union, Washington, D.C., pp. 71–98.

Topping, D.J., Rubin, D.M., Vierra Jr., L.E., 2000a. Colorado River sediment transport 1. Natural sediment supply limitation and the influence of Glen Canyon Dam. Water Resources Research 36, 515–542.

Topping, D.J., Rubin, D.M., Nelson, J.M., Kinzel III, P.J., Corson, I.C., 2000b. Colorado River sediment transport 2. Systematic bed-elevation and grain-size effects of sand supply limitation. Water Resources Research 36, 543–570.

Topping, D.J., Schmidt, J.C., Vierra Jr., L.E., 2003. Computation and analysis of the instantaneous-discharge record for the Colorado River at Lees Ferry, Arizona — May 8, 1921, through September 30, 2000. U.S. Geological Survey Professional Paper, vol. 1677.

Topping, D.J., Rubin, D.M., Schmidt, J.C., 2005. Regulation of sand transport in the Colorado River by changes in the surface grain size of eddy sandbars over multi-year timescales. Sedimentology 52, 1133–1153.

Topping, D.J., Rubin, D.M., Schmidt, J.C., Hazel Jr., J.E., Melis, T.S., Wright, S.A., Kaplinski, M., Draut, A.E., Breedlove, M.J., 2006a. Comparison of sediment-transport and bar-response results from the 1996 and 2004 controlled-flood experiments on the Colorado River in Grand Canyon. CD-ROM Proceedings of the 8th Federal Inter-Agency Sedimentation Conference, Reno, NV, April 2–6, 2006. ISBN: 0-9779007-1-1.

Topping, D.J., Wright, S.A., Melis, T.S., Rubin, D.M., 2006b. High-resolution monitoring of suspended-sediment concentration and grain size in the Colorado River using laser-diffraction instruments and a three-frequency acoustic system. CD-ROM Proceedings of the 8th Federal Inter-Agency Sedimentation Conference, Reno, NV, April 2–6, 2006. ISBN: 0-9779007-1-1.

Webb, R.H., Schmidt, J.C., Marzolf, G.R., Valdez, R.A. (Eds.), 1999. The 1996 controlled flood in Grand Canyon. American Geophysical Union, Washington, D.C. Geophysical Monograph, vol. 110.

Wiberg, P.L., Rubin, D.M., 1989. Bed roughness produced by saltating sediment. Journal of Geophysical Research (Oceans) 90, 5011–5016.

Wiberg, P.L., Smith, J.D., 1987. Calculations of the critical shear stress for motion of uniform and heterogeneous sediments. Water Resources Research 23, 1471–1480.

Wiberg, P.L., Smith, J.D., 1989. Model for calculating bed load transport of sediment. Journal of Hydraulic Engineering 115, 101–123.

Wilson, R.P., 1986. Sonar patterns of the Colorado River bed, Grand Canyon. Proceedings of the 4th Federal Inter-Agency Sedimentation Conference, Las Vegas, NV, March 24–27, 1986, pp. 5/133–5/142.

Wong, F.L., Anima, R.J., Galanis, P., Codianne, J., Xia, Y., Bucciarelli, R., Hamer, M., 2003. Grand Canyon riverbed sediment changes, experimental release of September 2000; a sample data set. U.S. Geological Survey Open-File Report 03-0265.

Wright, S., Parker, G., 2004. Density stratification effects in sand-bed rivers. Journal of Hydraulic Engineering 130, 783–795.

Wright, S.A., Melis, T.S., Topping, D.J., Rubin, D.M., 2005. Influence of Glen Canyon Dam operations on downstream sand resources of the Colorado River in Grand Canyon. In: Gloss, S.P., Lovich, J.E., Melis, T.S. (Eds.), The State of the Colorado River Ecosystem in Grand Canyon. U.S. Geological Survey Circular, vol. 1282, pp. 17–31.